Neurobiology of Aging 77 (2019) 66–86

Contents lists available at ScienceDirect

Neurobiology of Aging

journal homepage: www.elsevier.com/locate/neuaging

Prenatal noise stress aggravates cognitive decline and the onset and progression of beta amyloid pathology in a mouse model of Alzheimer's disease

Zahra Jafari [a,b], Megan Okuma [a], Hadil Karem [a], Jogender Mehla [a], Bryan E. Kolb [a,*], Majid H. Mohajerani [a,**]

[a] Department of Neuroscience, Canadian Centre for Behavioural Neuroscience (CCBN), University of Lethbridge, Lethbridge, Alberta, Canada
[b] Department of Basic Sciences in Rehabilitation, School of Rehabilitation Sciences, Iran University of Medical Science (IUMS), Tehran, Iran

ARTICLE INFO

Article history:
Received 17 June 2018
Received in revised form 8 January 2019
Accepted 21 January 2019
Available online 30 January 2019

Keywords:
Prenatal stress
Alzheimer's disease
Aβ plaque
Cognitive decline
Motor impairment
Prepulse inhibition
HPA axis
noise

ABSTRACT

Environmental distresses occurring during the sensitive periods of early life may exacerbate the vulnerability to develop physical and mental diseases in old age. Studies have shown the impact of prenatal stress (PS) on the endocrine development and reprogramming of hypothalamic-pituitary-adrenal axis functions in association with cognitive development and susceptibility to neuropsychiatric diseases. Long-term exposure to glucocorticoids can damage the brain and intensify the progression of Alzheimer's disease (AD)-like neuropathological changes, especially in females. There is, however, less information as to the link between PS and the risk of developing AD pathology throughout the lifespan. In the present study, male and female $APP^{NL\text{-}G\text{-}F/NL\text{-}G\text{-}F}$ offspring of dams exposed to gestational noise stress were compared with the control offspring in corticosterone alternations, cognitive and motor performances, and the onset age and development of amyloid beta (Aβ) plaques across age. The hyperactivity of the hypothalamic-pituitary-adrenal axis, spatial learning, and Aβ development were sex specific, showing persistent high levels of stress and further memory loss in females than males, especially in PS mice. The Aβ deposition was started earlier, by 2–3 months, and exhibited a heightened progression in PS animals. The PS also created a long-lasting anxiety-like behavior and impairment in cognitive function and motor coordination. Our results suggested PS as a risk to exacerbate AD-like neuropathological changes during the lifespan, with higher susceptibility of females. The findings were discussed in line with the most likely mechanisms for the PS effects, that is, dysregulation of the neuroendocrine system and the placenta by the PS.

1. Introduction

Besides extensive experimental animal studies, epidemiological and mechanistic human research have shown that prenatal stressors are the most impressive early environmental factors in offspring development and susceptibility to diseases and mental health problems in old age (Hoeijmakers et al., 2017; Van den Bergh et al., 2017). Prenatal stress (PS) or exposure to glucocorticoids during sensitive periods of development has an organizational effect on biological systems (i.e., the central nervous system, autonomic nervous system, neuroendocrine axis [hypothalamic-pituitary-adrenal {HPA} axis], cardiovascular, and immune systems), and systematically pose a potential risk factor for multiple neuropsychiatric disorders and mental illnesses during the lifespan (Abbott et al., 2018; Van den Bergh et al., 2017). Evidence for epigenetic programming of the endocrine system induced by stress experienced during early gestation indicates that the PS can result in alterations of DNA-methylation at corticotropin-releasing hormone (CRH) and glucocorticoid receptor (GR) gene promoters. These epigenetic variations create persistent changes in central CRH and GR expression related to HPA-axis hyper-responsivity and may last into adulthood and even continue to the next generation (Bock et al., 2015; Crudo et al., 2012).

Alzheimer's disease (AD), the most widespread neurodegenerative disease among elderly, accounts for 60%–80% of dementia cases (Cui and Li, 2013; Marcello et al., 2015). It is characterized by a

* Corresponding author at: Department of Neuroscience, Canadian Centre for Behavioural Neuroscience (CCBN), University of Lethbridge, Lethbridge, Alberta, Canada, T1K 3M4. Tel.: +403 329 2405; fax: +403 329 2775.
** Corresponding author at: Department of Neuroscience, Canadian Centre for Behavioural Neuroscience (CCBN), University of Lethbridge, Lethbridge, Alberta, Canada, T1K 3M4. Tel.: +403 394 3950; fax: +403 329 2775.
E-mail addresses: kolb@uleth.ca (B.E. Kolb), mohajerani@uleth.ca (M.H. Mohajerani).

0197-4580/$ – see front matter © 2019 Elsevier Inc. All rights reserved.
https://doi.org/10.1016/j.neurobiolaging.2019.01.019

progressive deterioration of cognitive functions and the accumulation of specific neuropathological hallmarks, such as various extracellular beta amyloid (Aβ) peptides and neurofibrillary tangles made up of hyperphosphorylated tau inside of neurons, as well as neuronal and synaptic loss in the cerebral cortex and hippocampus (Cui and Li, 2013; Hoeijmakers et al., 2018; Marcello et al., 2015). Although the complex etiology of the AD is not fully understood, the effects of lifestyle characteristics, environmental factors, sex, and dysregulation in epigenetic, nervous system, neuroendocrine, and immune system mechanisms in the risk of developing AD-like pathology have been tackled in multiple multidisciplinary studies (Carroll et al., 2010; Cui and Li, 2013; Hoeijmakers et al., 2018; Jafari et al., 2018a,b; Khalsa, 2015; Livingston et al., 2017).

Noise as a common environmental health hazard is more than just a nuisance (Basner et al., 2014). Among well-known risk factors related to lifestyle for mental disease and AD, noise stress (Cui and Li, 2013; Ouis, 2001) is an inherent component of modern life that has a major contribution in shaping the brain and behavior (Belnoue et al., 2016; Jafari et al., 2017b; Marcello et al., 2015). Stress also has been shown to have a causative relationship with various risk factors for the AD (Khalsa, 2015; Livingston et al., 2017). Although human evidence supports biological correlates of PS with deviations in neurodevelopment, neurocognitive function, neuronal processing, functional and structural brain connectivity in limbic cortex, and dysregulations in HPA axis and autonomous nervous system (Van den Bergh et al., 2017; Zijlmans et al., 2015), current experimental evidence also collectively points to the negative impacts of stress as a risk factor for precipitating AD-like neuropathological changes in rodents (Cui and Li, 2013; Marcello et al., 2015). For instance, the impact of stress during adulthood on exacerbation of Aβ accumulation, hyperphosphorylated tau, neuroinflammation, and cognitive decline (Cuadrado-Tejedor et al., 2012; Cui et al., 2012; Jafari et al., 2018b), as well as PS-induced sex-specific alterations of N-methyl-D-aspartate receptor (Fang et al., 2018) as a key mediator of Aβ synaptotoxicity, higher levels of hippocampal brain-derived neurotrophic factor (BDNF) and increased Aβ pathology (Fang et al., 2018; Sierksma et al., 2012), and higher hippocampal plaque load and altered amyloid precursor protein (APP) processing in the CA3 (Sierksma et al., 2013) all have been reported.

Although (1) the link between stress experienced in utero and later deficits in memory, learning ability, social behavior, alterations in stress regulation, and higher vulnerability to adult diseases has been indicated in both humans and rodent models (Antonelli et al., 2017; Neigh et al., 2017; Weinstock, 2017), (2) Aβ dyshomeostasis has emerged as the most extensively validated hypothesis associated with cognitive impairment in AD pathology among diverse factors contributed to AD pathogenesis (Selkoe and Hardy, 2016), and (3) dysregulation of the maternal and fetal HPA axes have been shown as the most likely candidates for the negative effects of PS on brain development and increased susceptibility to neuropsychiatric and brain diseases in old age (Charil et al., 2010; Maccari et al., 2003; Weinstock, 2017), no experimental study has examined what the link between PS-induced HPA-axis hyperactivity and the onset and progression of Aβ pathology is or how it is modulated by age and sex during the lifespan. Our study was novel in (1) using a gestational noise stress paradigm as a lifestyle risk factor for AD common today (Cui and Li, 2013; Marcello et al., 2015); (2) probing for the onset and progression of Aβ pathology in cortical, subcortical, and limbic brain areas; (3) applying a set of behavioral tests sensitive to learning, memory, motor performance, and anxiety-like behavior; (4) probing for changes in HPA axis responsivity, behavior, and Aβ pathology in both sexes during the lifespan; and (5) using a unique AD mouse model ($APP^{NL\text{-}G\text{-}F/NL\text{-}G\text{-}F}$), which represents age-dependent changes in the brain and behavior. The knock-in $APP^{NL\text{-}G\text{-}F/NL\text{-}G\text{-}F}$ mouse is a second-generation mouse model of AD that was recently developed at the Riken Institute in Japan (Saito et al., 2014; Sasaguri et al., 2017). It has a modified *APP* gene that has humanized Aβ sequence with 3 mutations (Swedish, Beyreuther/Iberian, and Arctic) in $APP^{NL\text{-}G\text{-}F}$. This mouse model produces a robust age-related spread of Aβ aggregates and cognitive deficits titrated to endogenous levels of APP with no sign of tauopathy. The cortical deposition specifically starts after 2 months and is almost saturated by 7 months. Subcortical amyloidosis is also shown after 4 months (Jafari et al., 2018b; Saito et al., 2014). Because APP is not overproduced in human AD, this last point provides an important improvement over earlier Aβ-based mouse models of AD (Sasaguri et al., 2017). Earlier mouse models overexpressed APP or APP-presenilin 1 (PS1), which led to the accumulation of unusual fragments generated by α-secretase, such as C-terminal fragment-β. C-terminal fragment-β is more toxic than Aβ and does not accumulate in human AD brains (Saito et al., 2016; Sasaguri et al., 2017). Thus, in this mouse model of AD, we aimed to determine how PS modulates HPA-axis responsivity, onset, and progression of Aβ pathology and also learning, memory, anxiety-like behavior, and motor coordination during the lifespan.

2. Material and methods

2.1. Animals

The male and female pairs of AD transgenic mice carrying Swedish (NL), Arctic (G), and Beyreuther/Iberian (F) mutations ($APP^{NL\text{-}G\text{-}F/NL\text{-}G\text{-}F}$) were provided by RIKEN Brain Science Institute, Japan. Then, a colony of $APP^{NL\text{-}G\text{-}F/NL\text{-}G\text{-}F}$ mice was maintained at the Canadian Center for Behavioural Neuroscience. Thirty-two female $APP^{NL\text{-}G\text{-}F/NL\text{-}G\text{-}F}$ mice at 8 weeks of age were individually mated with 32 male $APP^{NL\text{-}G\text{-}F/NL\text{-}G\text{-}F}$ mice in standard shoe-box cages. For the recording of the gestational length, a former protocol was followed (Jafari et al., 2017a,d). At the age of 22–23 days, the pups were weaned from their mothers. All animals were given access to food and water ad libitum and were maintained on a 12:12-h light:dark cycle. All testing and training was performed during the light phase of the cycle at the same time of day. The experimental procedures were approved by the University of Lethbridge Animal Care Committee in compliance with the standards set out by the Canadian Council for Animal Care.

2.2. Experimental design

Pregnant mice were randomly assigned to 2 groups consisting of one stress group and one control group (CG). We exposed animals to stress on gestational days (GDs) 12–16 because the corticogenesis process occurs from embryonic day 10–17 in mice, and layers II/III, IV, and V mainly develop during GDs 12-16 (Kolb et al., 2012, 2013). This timeframe also corresponds to the second trimester of human pregnancy when substantial neural development occurs (Clancy et al., 2007).

2.2.1. Noise stress procedure

The noise stress paradigm consisted of an intermittent 3000 Hz frequency sound of 90 dB for 1 second duration and 15-second interstimulus interval (Jafari et al., 2017a). On GDs 12, 14, and 16, the mice ($n = 16$) in groups of 2 to 3 in their standard cage were moved to a sound chamber specified for the stress group. A speaker, which emitted the noise stimulus, was placed inside the cage. The sound pressure level was monitored daily inside the cage without an animal (Tektronix RM3000, Digital Phosphor Oscilloscope). The mice were exposed to the noise stress for 24 hours starting at 8:00 am (Jafari et al., 2018b). We used a 3000 Hz frequency tone because

(1) it is audible to mice (Heffner and Heffner, 2007) and (2) it is relatively similar to environmental and traffic noises which are largely made up of low frequency to midfrequency tones (Chang et al., 2014). We applied an intermittent stimulus intensity to prevent noise-induced hearing loss. Twenty-four hours of rest after every stress exposure also provides enough time for recovery from possible temporary threshold shifts (White et al., 1998).

2.2.2. Control group

Pregnant mice (n = 16) on GDs 12, 14, and 16 in groups of 2 to 3 in their standard cage were moved to a sound chamber specified for the CG. A silent speaker was placed inside the cage. The mice were left undisturbed for 24 hours starting at 8:00 am. In the CG, no stress was given.

2.3. Plasma corticosterone assay

Blood was taken from the submandibular vein at 7:30 to 8:30 am a day before starting behavioral tests at ages 2, 6, and 10 months. Approximately 0.1 mL of blood was collected in heparin-coated tubes. The tubes were centrifuged at 6000 rpm at 4 °C for 15 minutes to collect the plasma. Collected plasma samples were stored at −80 °C and then analyzed as previously described (Jafari et al., 2018a,b).

2.4. Behavioral tests

Several behavioral tests were performed across age 2, 6, and 10 months to measure the effect of PS on cognitive and motor performance of the offspring. Tests of prepulse inhibition (PPI) of the acoustic startle reflex (ASR), novel object recognition (NOR), rotarod (RR), balance beam test, and the Morris water task (MWT) were conducted, respectively, in separate days, with an alternating order of animals by the same examiner in the mornings at 8–11 am (Fig. 1).

2.4.1. Prepulse inhibition of the acoustic startle reflex

The PPI of the ASR is one of the well-known experimental paradigms in the field of neuropsychiatric disorders (Koch, 1999; Li et al., 2009). The PPI implies a normal reduction of the amplitude of the startle reflex when a weak prepulse stimulus is presented 30–500 msec before the startling stimulus. Thus, the PPI is used as an index of sensorimotor gating (Rohleder et al., 2014). Animal studies suggest that the sensorimotor gating is impaired with the progressing of AD pathology, and its abnormalities may be linked to cognitive impairment and cerebral Aβ neuropathology (Wang et al., 2012). Stress is also known to modulate the PPI. Impairments in sensorimotor gating have been reported after stress exposure (Bakshi et al., 2012; Conti and Printz, 2003; Jafari et al., 2018a,b; Kjaer et al., 2010), social isolation (Bailoo et al., 2016; Chang et al., 2014), variation in maternal care (Cromwell and Atchley, 2015), or corticotropin-releasing factor injection (Bakshi et al., 2012; Conti et al., 2002) in rodents and also subsequent to performing a stressful task (performing a complex task with time restriction) (De la Casa et al., 2016) or cortisol injection (Richter et al., 2011) in humans. In our study, each mouse was placed in a plastic cylinder situated on a plate with a pressure sensor in an acoustic chamber (PANLAB Harvard Apparatus). Any animal motion was detected by the sensor which measured its amplitude and stored data on a computer hard drive. Software generated a sequence of stimulus trials including a startle stimulus, a prepulse stimulus, and a startle stimulus paired with a prepulse stimulus in a white background noise of 65 dB. The ASR stimulus was an 8 kHz tone frequency with 115 dB intensity, 40 ms duration, and a 1 ms rise/fall time. The prepulse stimulus was also an 8 kHz tone frequency with 80 dB intensity, 20 ms duration, and a 1 ms rise/fall time, which was presented 100 ms before the startle stimulus. The testing session was started with an acclimation period lasting 3 minutes. Then the animals received 10 startle-only trials to habituate their startle responses to a steady state level. Immediately afterward, forty trials including 10 “no stimulus,” 10 “pulse stimulus,” 10 “prepulse stimulus,” and 10 “prepulse + pulse stimulus” were presented in a pseudorandom order with 30 seconds of interstimulus interval. The PANLAB system automatically presented the ASR and PPI (%) in an Excel data spreadsheet. The PPI ratio was calculated by subtracting the ASR amplitude from the PPI amplitude divided by the ASR amplitude multiplied 100 (Jafari et al., 2018a,b).

2.4.2. Novel object recognition test

Each mouse was placed in an open-field arena made of white Plexiglas. In the first trial, the mouse was placed in the arena with 2 identical objects and was allowed to explore the field for 5 minutes. The animal was removed and placed in a transport box for 3 minutes, and one of the objects was randomly replaced with a new object. The mouse was then returned to the arena, and the animal’s exploration was filmed for 3 minutes. The time spent with each object (sec) and the ratio of time spent with the old compared with the new object (calculated by subtracting times spent with old from the new object divided by the total time spent for exploration) were measured during the second session. In addition, behavioral measures including movement time (the time in seconds spent moving in the arena), movement number (the number of movements after the animal remained immobile for more than one second), total distance (the total length of paths traveled by animals, in centimeters), and rest time (the time in seconds spent immobile) during the second session were calculated to determine the locomotor behavior of the animals (Jafari et al., 2017d).

2.4.3. Elevated plus maze test

The elevated plus maze has been constructed from black Plexiglas. The maze was housed in an empty room, and a dim light was used during filming. Each mouse was filmed for 5 minutes and manually scored for time spent in the open arms (sec), time spent in the closed arms (sec), number of entries to either the open arms or closed arms, and the ratio of the number of entries to closed arms versus the open arms (calculated by subtracting number of entries to closed arms from the number of entries to open arms divided by the total number of entries to closed and open arms) (Jafari et al., 2017a, 2018a).

2.4.4. Rotarod test

Animals were briefly pretrained on an automated 4-lane RR treadmill (ENV-575M Mouse, Med Association Inc). For the protocol, mice were placed into individual sections of the RR and tested at 2 constant speeds (8 rpm and 16 rpm) on separate days. Each animal’s performance score in seconds was recorded when the mouse was unable to stay on the RR, trips a plate, and stops the timer. Mice were subjected to 2 trials, with a maximum time of 3 minutes and a 5-minute intertrial test interval. Two trials per animal were averaged (Jafari et al., 2018a,b).

2.4.5. Balance beam test

The mice were required to traverse an elevated, narrow aluminum beam (1 cm diameter, 100 cm long, and 50 cm above a foam pad) to reach an enclosed escape box. Mice were first trained (3-4 trials) and were tested (3 trials) on the next day. The mean latency (sec), distance traveled (cm), and number of foot slips across the 3 testing trials were manually scored (Jafari et al., 2017a, 2018b).

2.4.6. Morris water task

The water task consisted of a pool (153 cm diameter) filled with water (23 °C–25 °C) up to a level of ~15 cm from the top edge of the tank. The water was made opaque by nontoxic white tempera

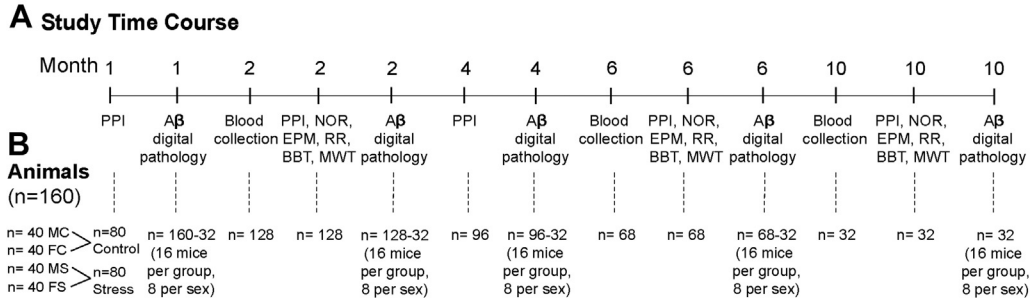

Fig. 1. Section A demonstrates the time of each procedure across age in $APP^{NL-G-F/NL-G-F}$ offspring, and section B shows the number of animals per procedure. Blood collection was performed before running 6 behavioral tests, that is, PPI of the ASR, NOR, EPM, RR, BBT, and MWT, at 2, 6, and 10 months. For probing the onset age, distribution (%), and size (μm) of Aβ plaques, an identical number of offspring per sex were included at 5 ages 1, 2, 4, 6, and 10 months in each group (n = 160, n per group = 80, n per sex = 40). Abbreviations: Aβ, amyloid beta; ASR, acoustic startle reflex; BBT, balance beam test; EPM, elevated plus maze; MWT, Morris water task; NOR, novel object recognition; PPI, prepulse inhibition; RR, rotarod.

paint. The pool was located in a room rich with distal cues. During all hidden platform trials, the platform was submerged ~1.0 cm under the surface of the water. The tank was divided virtually into 4 quadrants, with starting points at north, west, east, and south. Animals were trained with 4 trials per day for 8 consecutive days (Water 2100 software vs. 7, 2008). Each trial began with the mouse being placed in the pool in a pseudorandom sequence at one of the 4 cardinal compass positions around the perimeter of the pool. Testing was stopped after the mouse reached the platform or if the mouse did not find the platform, at the 60-second trial time limit. Data were recorded using an automated tracking system (HVS Image, Hampton, U.K.). The swim time (sec), swim speed (m/s), and swim distance (m) were calculated for analysis. The probe trial was also carried out on the ninth day, 24 hours after the last acquisition trial, in which the platform was removed, and each mouse was allowed to swim freely for 60 seconds. The time spent in the quadrant where the platform had been located was measured (Jafari et al., 2017c, 2018b).

2.5. Quantification of the Aβ plaque area

2.5.1. Methoxy-X04 injection and brain imaging

Methoxy-X04 is a fluorescent dye that selectively binds to β-pleated sheets found in dense core Aβ plaques. It has high specificity in staining Aβ plaques in postmortem sections of the AD brain (Hefendehl et al., 2011). The methoxy-X04 solution was prepared by dissolving the Methoxy into a solution containing 10% dimethyl sulfoxide, 45% propylene glycol, and 45% sodium phosphate buffered saline (Bisht et al., 2016). Twenty-four hours before perfusion at ages 1, 2, 4, 6, and 10 months, mice were weighed and given an intraperitoneal injection of methoxy-X04 at a dose of 10 mg/kg of body weight. Then they were euthanized via a transcardiac perfusion of 0.9% saline followed by paraformaldehyde. Brains were removed and postfixed for 24 h in paraformaldehyde. They were subsequently sliced at 50 μm using a Cryostat, and every second section was mounted on glass slides. The brain sections were scanned by NanoZoomer (Hamamatsu Photonics, Japan), and images were used for quantification of Aβ plaque areas (PAs) (%) (Saito et al., 2014). The animals' endpoints were considered according to the development of Aβ pathology in our mouse model of AD (Jafari et al., 2018b; Saito et al., 2014). The same animals that were used in the behavioral tests were also used for the histological analyses. The animals were sacrificed after blood collection and completing all behavioral tests (Fig. 1) before each endpoint. The experimenter was blind to the experimental groups.

2.5.2. Brain sections and regions of interests

For each brain, 6 coronal sections (Bregma ~3.20, 2.96, 0.98, −2.06, −3.08, and −5.34 mm) corresponding with a mouse brain atlas (Paxinos, 2001) were selected for quantifying Aβ PAs (Jafari et al., 2018b; Saito et al., 2014) (Figs. 4 and 5; Fig. S2). In each brain section, the total Aβ PA was computed. Quantification was also performed for some specific brain regions that studies have shown to be involved in AD progression, stress handling, or in the regulation of brain cognitive processes (Charil et al., 2010; Huizink et al., 2004; Jafari et al., 2018b; Kim et al., 2015; Saar et al., 2015). Each brain section was uploaded in ImageJ 1.4.3.67 software, and the Aβ PA (%) of the region of interest (ROI) was determined via using required image processing options under Edit, Image, Process, and Analyze tabs. The ROIs were frontal pole (FP), olfactory area (OA), isocortex (IC), anterior cingulate area (ACA), nucleus accumbens (NA), hippocampal region (HR), posterior parietal area (PPA), retrosplenial area (RA), entorhinal area, cortical amygdalar area (CAA), a midbrain (MB), and hindbrain (HB). These 6 coronal sections were chosen to measure the Aβ PA as they provided a good view for differentiating selected ROI's boundaries. The largest plaque size (μm) was also measured in each brain section.

2.6. Statistical analysis

All statistical analyses were performed using SPSS Statistics 24.0 at a significance level of ≤ 0.05. Normally distributed data were analyzed using the Kolmogorov–Smirnov test. Univariate analysis of variance was conducted to compare the groups regarding different parameters of the corticosterone assay, behavioral tests, and Aβ plaque measurements. A repeated measures ANOVA was used for all comparisons across age in each group. The interaction of age and PS was assessed by conducting two-way ANOVAs in all measures, that is, corticosterone levels, behavioral tests, and Aβ plaque quantifications. The F values, degrees of freedom, p values, estimations of the effect size (partial η^2), and observed power have been reported for the statistical analyses. Adjustment for multiple comparisons of group means in each measurement was performed with Bonferroni correction.

3. Results

There was a significant difference between the 2 sexes in corticosterone levels, the MWT, and Aβ plaque measurements. In other behavioral tests, no sex effect was observed ($p \geq 0.205$). Thus, the sex analysis only has been reported on the measures in which it was significant.

3.1. The PS impact on corticosterone levels

The corticosterone level was significantly higher in the PS groups compared with the CGs over age (2 months: $F_{3,124} = 14.161$, $p \leq 0.001$; 6 months: $F_{3,64} = 12.943$, $p \leq 0.001$; 10 months:

$F_{3,28} = 7.761$, $p = 0.004$). Females showed higher corticosterone levels than males across age. The sex effect was significant in the PS group (2 months: $p = 0.019$; 6 months: $p = 0.037$; 10 months: $p = 0.041$) (Fig. 2A1, Table 1). Fig. 2A2 exhibits the trend of changes in corticosterone levels across age that was not significant in each group (Table 2).

3.2. The PS impact on cognitive function and motor coordination

3.2.1. Prepulse inhibition of the acoustic startle reflex

The ASR amplitude (%) was almost identical in the 2 groups over age (Fig. 2B1). The PS group revealed a significant reduction of the PPI amplitude at all ages, except one month, compared with the CG (2 months: $F_{1,126} = 10.695$, $p = 0.002$; 4 months: $F_{1,94} = 10.879$, $p = 0.002$; 6 months: $F_{1,66} = 8.222$, $p = 0.007$; 10 months: $F_{1,30} = 0.096$, $p = 0.005$) (Fig. 2B2, Table 3). The ASR latency (ms) increase by age was almost the same in both groups (Fig. 2B3), whereas the PS groups displayed a significantly higher PPI latency than the CG at 2, 6, and 10 months (2 months: $F_{1,126} = 9.535$, $p = 0.004$; 6 months: $F_{1,66} = 10.017$, $p = 0.006$; 10 months: $F_{1,30} = 9.316$, $p = 0.009$) (Fig. 2B4, Table 3). The highest ASR and PPI amplitudes were shown at 2 and 4 months in both groups, respectively. The age effect was significant for the 2 groups in all measures (*CG*: ASR amplitude: $F_{4,48} = 5.152$, $p = 0.001$; PPI amplitude: $F_{4,48} = 23.873$, $p \leq 0.001$; ASR latency: $F_{4,48} = 7.276$, $p \leq 0.001$; PPI latency: $F_{4,48} = 11.309$, $p \leq 0.001$; *PS group*: ASR amplitude: $F_{4,48} = 6.387$, $p \leq 0.001$; PPI amplitude: $F_{4,48} = 3.59$, $p = 0.009$; ASR latency: $F_{4,48} = 6.903$, $p \leq 0.001$; PPI latency: $F_{4,48} = 8.02$, $p \leq 0.001$) (Table 4).

3.2.2. Novel object recognition test

The amount of exploration time spent with the 2 identical objects in the first trial was similar in the 2 groups (Table 3). The PS group exhibited a significantly lower new object time and higher ratio of old object time (NOR ratio) compared with the CG across age (2 months: $F_{1,126} = 4.319$, $p = 0.042$; 6 months: $F_{1,66} = 19.88$, $p \leq 0.001$; 10 months: $F_{1,30} = 15.648$, $p = 0.001$) (Fig. 2C1 and C3). The

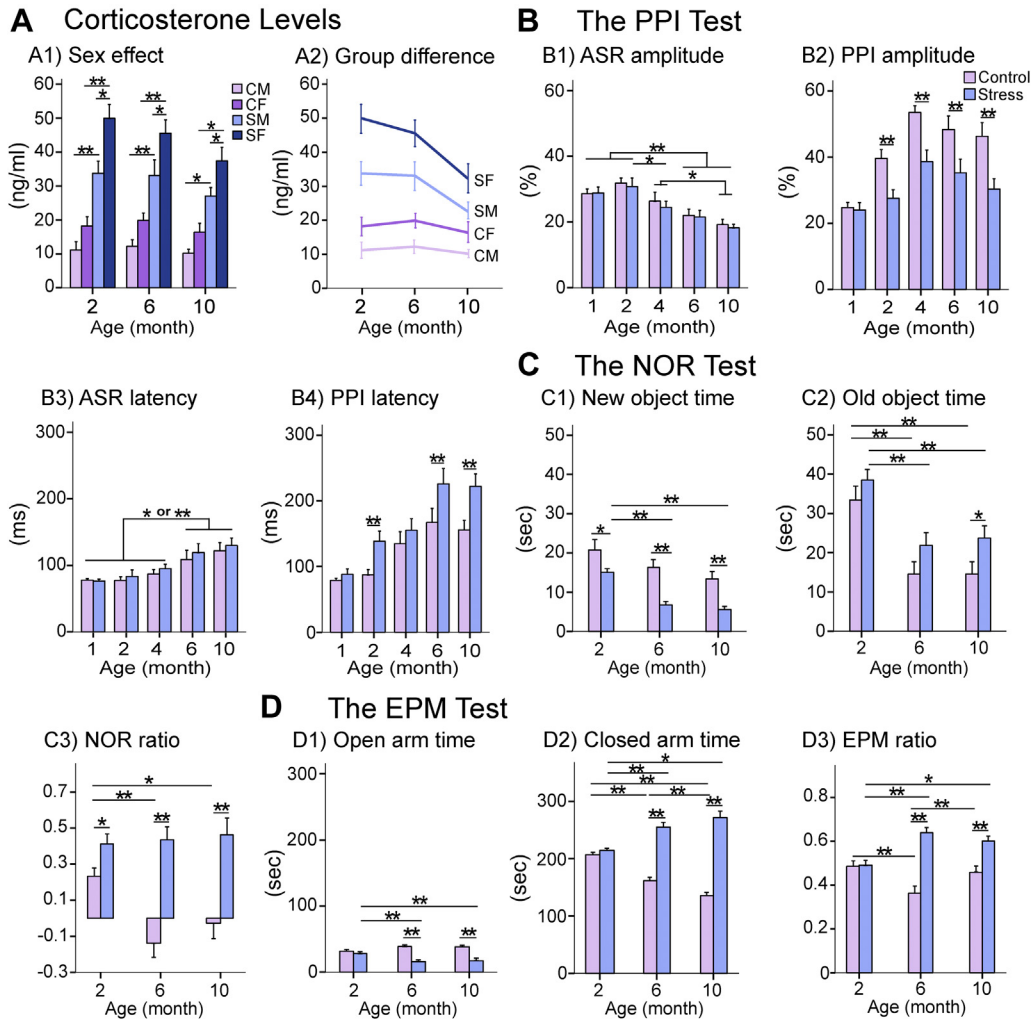

Fig. 2. Results of the corticosterone assay and behavioral tests. (A) The corticosterone levels (ng/mL): (A1) The corticosterone level was significantly higher in the PS group compared with the CG in both sexes over age. The sex effect was significant in the PS group. (A2) The trend of changes in corticosterone levels across age. The age effect was not significant. (B) The PPI of the ASR test: (B1) The ASR amplitude (%) significantly decreased by age in both groups. (B2) The PPI amplitude (%) was significantly lower in the PS group than the CG, except at 1 month. (B3 and B4) The ASR and PPI latencies (ms) increased by age in both groups. The stress group exhibited a significantly higher PPI latency than the CG at 2, 6, and 10 months. The age effect was significant in all measures (Table 4). (C) The NOR test: (C1) The PS group showed a significantly shorter new object time (sec) and (C2) longer old object time (sec). (D) The EPM test: a significantly shorter open arm time (D1), longer closed arm time (D2), and lower number of entries to open arm (D3) in the PS group than the CG at 6 and 10 months. The adverse effect of age on all measures was observed in the PS group (Table 2). Results reported as mean ± SEM. Asterisks indicate $^{*}p < 0.05$ or $^{**}p < 0.01$. Abbreviations: CF, control female; CG, control group; CM, control male; EPM, elevated plus maze; NOR, novel object recognition; PPI of the ASR, prepulse inhibition of the acoustic startle reflex; PS, prenatal stress; SF, stress female; SM, stress male.

Table 1
Comparing the PS and control groups in corticosterone levels and the MWT's measures

Tests/ Measurements	Between groups' p-values[c]				Significant main effects[d]			
	CM, SM	CF, SF	CM, CF	SM, SF	$F_{dfn,dfd}$	p	η^2	Power
Corticosterone levels (ng/mL)								
2 mo	≤0.001[b]	≤0.001[b]	0.272	0.019[a]	$F_{3,124} = 14.161$	≤0.001[b]	0.612	1.000
6 mo	0.002[b]	≤0.001[b]	0.254	0.037[a]	$F_{3,64} = 12.943$	≤0.001[b]	0.663	1.000
10 mo	0.031[a]	0.011[a]	0.327	0.041[a]	$F_{3,28} = 7.761$	0.004[b]	0.582	0.971
MWT								
Latency (s) at 2 mo	0.189	0.133	0.418	0.580	$F_{3,124} = 1.522$	0.207	0.003	0.405
Distance (m) at 2 mo	0.142	0.105	0.716	0.317	$F_{3,124} = 1.506$	0.215	0.005	0.683
Probe time (%) at 2 mo	0.752	0.803	0.785	0.810	$F_{3,124} = 0.147$	0.931	0.008	0.075
Latency (s) at 6 mo	0.021[a]	≤0.001[b]	0.031[a]	≤0.001[b]	$F_{3,64} = 13.323$	≤0.001[b]	0.073	1.000
Distance (m) at 6 mo	0.010[a]	≤0.001[b]	0.042[a]	≤0.001[b]	$F_{3,64} = 16.941$	≤0.001[b]	0.064	1.000
Probe time (%) at 6 mo	0.046[a]	0.040[a]	0.360	0.211	$F_{3,64} = 4.964$	0.011[a]	0.317	0.812
Latency (s) at 10 mo	0.006[b]	≤0.001[b]	0.231	0.005[b]	$F_{3,28} = 12.861$	≤0.001[b]	0.064	1.000
Distance (m) at 10 mo	≤0.001[b]	≤0.001[b]	0.178	≤0.001[b]	$F_{3,28} = 22.575$	≤0.001[b]	0.107	1.000
Probe time (%) at 10 mo	0.042[a]	0.039[a]	0.401	0.377	$F_{3,28} = 4.357$	0.041[a]	0.393	0.681

Key: ANOVA, analysis of variance; MWT, Morris water task; CF, control female; CM, control male; dfd (N-G), degrees of freedom denominator; dfn (G-1), degrees of freedom numerator; Partial η^2, an estimate of effect size; PS, prenatal stress; SF, stress female; SM, stress male.
Univariate ANOVAs were used for statistical analyses.
[a] $p < 0.05$.
[b] $p < 0.01$.
[c] The "between groups' p-values" show p-values for the between-group comparisons.
[d] The "significant main effects" indicate the statistical results of a significant main effect for every measure.

old object time was significantly longer at 10 months in the PS group ($F_{1,30} = 4.587$, $p = 0.037$) (Fig. 2C2, Table 3). New object time significantly decreased by age only in the PS group ($F_{2,30} = 13.367$, $p \leq 0.001$). The old object time was significantly shorter for both groups at higher ages (CG: $F_{2,30} = 11.133$, $p \leq 0.001$; PS group: $F_{2,30} = 8.298$, $p \leq 0.001$) (Table 2). No significant difference was observed between the 2 groups on any measures of the locomotion behavior across age.

3.2.3. Elevated plus maze test

The PS group showed a significantly shorter open arm time (6 months: $F_{1,66} = 34.628$, $p \leq 0.001$; 10 months: $F_{1,30} = 21.164$, $p \leq 0.001$), longer closed arm time (6 months: $F_{1,66} = 83.861$, $p \leq 0.001$; 10 months: $F_{1,30} = 77.731$, $p \leq 0.001$), lower number of entries to open arms (6 months: $F_{1,66} = 43.683$, $p \leq 0.001$; 10 months: $F_{1,30} = 11.442$, $p = 0.003$), and higher ratio of the number of entries to closed arms (6 months: $F_{1,66} = 48.902$, $p \leq 0.001$; 10 months: $F_{1,30} = 9.533$, $p = 0.005$) than the CG (Fig. 2D, Table 3). The PS group also exhibited a significantly shorter open arm time ($F_{2,30} = 7.292$, $p = 0.002$), longer closed arm time ($F_{2,30} = 21.709$, $p \leq 0.001$), reduced number of entries to open arms ($F_{2,30} = 13.459$, $p \leq 0.001$), and higher ratio of the number of entries to closed arms across age ($F_{2,30} = 8.98$, $p \leq 0.001$). Closed arm time significantly decreased by age in the CG ($F_{2,30} = 52.846$, $p \leq 0.001$) (Table 2).

3.2.4. Rotarod test

The PS group exhibited an impaired performance in both RR speeds at 6 (8 rpm speed: $F_{1,66} = 4.665$, $p = 0.046$; 16 rpm speed: $F_{1,66} = 7.059$, $p = 0.013$) and 10 months (8 rpm speed: $F_{1,30} = 4.791$, $p = 0.044$; 16 rpm speed: $F_{1,30} = 4.771$, $p = 0.043$) (Fig. 3A, Table 3). Improvement in RR time by age was only observed in the CG (8 rpm speed: $F_{2,30} = 9.737$, $p \leq 0.001$; 16 rpm speed: $F_{2,30} = 3.937$, $p = 0.027$) (Table 2).

3.2.5. Balance beam test

The PS group spent a significantly longer time to pass across the beam (6 months: $F_{1,66} = 20.832$, $p \leq 0.001$; 10 months: $F_{1,30} = 10.504$, $p = 0.005$) and displayed a higher number of foot slips (6 months: $F_{1,66} = 41.501$, $p \leq 0.001$; 10 months: $F_{1,30} = 111.910$, $p \leq 0.001$) compared with the CG (Fig. 3B, Table 3). Latency ($F_{2,30} = 12.826$, $p \leq 0.001$) and number of foot slips ($F_{2,30} = 37.491$, $p \leq 0.001$) were significantly increased by age only in the PS group (Table 2).

3.2.6. Morris water task

The PS group demonstrated an increased latency (sec) (6 months: $F_{3,64} = 13.323$, $p \leq 0.001$; 10 months: $F_{3,28} = 12.861$, $p \leq 0.001$) and swim distance (m/s) (6 months: $F_{3,64} = 16.941$, $p \leq 0.001$; 10 months: $F_{3,28} = 22.575$; $p \leq 0.001$) compared with the CG (Fig. 3C1, Table 1). There was also a stress effect in which these measures were significantly larger in females than males at 6 months for the CG ($p \leq 0.042$) and ages 6 and 10 months in the PS group ($p \leq 0.001$). Improvement in swim latency by age due to a practice effect was not shown in the stress female group (Fig. 3C2, Table 2).

In the probe test, the same pattern of lower scores in the PS group than the CG was observed (6 months: $F_{3,64} = 4.964$, $p = 0.011$; 10 months: $F_{3,28} = 4.357$, $p = 0.041$) (Fig. 3C3, Table 1). A significantly impaired probe time by age was shown only in the female stress group ($F_{2,30} = 6.255$, $p = 0.005$) (Fig. 3C4, Table 2).

3.3. The PS impact on the onset and progression of Aβ plaques

The Aβ PA (%) was compared between the PS group and CG per sex. At 1 month, only a small number of plaques were shown in OA, especially in the glomerular layer of the main olfactory bulb (in 2–3 animals per group) and no significant difference was observed (Fig. S1). The PS groups exhibited a noticeable Aβ aggregation at 2 months and their differences with the CGs were significant in brain sections A1-A5 (A1: $F_{3,124} = 18.186$, $p \leq 0.001$; A2: $F_{3,124} = 7.264$, $p = 0.001$; A3: $F_{3,124} = 4.269$, $p = 0.015$; A4: $F_{3,124} = 7.264$, $p = 0.001$; and A5: $F_{3,124} = 4.102$, $p = 0.017$) and all specific brain areas (FP: $F_{3,124} = 40.621$, $p \leq 0.001$; OA: $F_{3,124} = 7.586$, $p = 0.001$; IC: $F_{3,124} = 24.451$, $p \leq 0.001$; ACA: $F_{3,124} = 4.178$, $p = 0.016$; PPA: $F_{3,124} = 7.472$, $p = 0.001$; RA: $F_{3,124} = 4.072$, $p = 0.018$) except for NA, HR, EA, CAA, MB, and HB (Fig. 4B, Table 5). The PS heightened Aβ accumulation and significantly increased the PA than the CGs in all brain sections (A1-A6) and specified brain regions at 4, 6, and 10 months (Figs. 4 and 5, Table 5).

There was also a sex effect, wherein a significantly higher PA was shown in the stress female group than the stress male group in total PA of all brain sections and also in specific brain regions FP, IC, ACA, RA, and HB at 6 months and the total PA in A6 at 10 months. The PA

Table 2
Statistical results of comparing the repeat of corticosterone assays and behavioral tests across age per group

Tests/ Measurements	Between groups' *p*-Values[c]			Significant main effects[d]			
	2, 6 mo	2, 10 mo	6, 10 mo	$F_{dfn,dfd}$	*p*	η^2	Power
Corticosterone levels (ng/mL)							
Control male	0.712	0.713	0.738	$F_{2,30} = 0.237$	0.791	0.024	0.082
Control female	0.719	0.689	0.469	$F_{2,30} = 0.274$	0.763	0.030	0.087
Stress male	0.928	0.170	0.196	$F_{2,30} = 1.221$	0.317	0.114	0.234
Stress female	0.593	0.062	0.115	$F_{2,30} = 2.348$	0.121	0.190	0.412
NOR in the CG							
New object time (s)	0.187	0.039[a]	0.437	$F_{2,30} = 2.413$	0.102	0.101	0.460
Old object time (s)	≤0.001[b]	≤0.001[b]	0.993	$F_{2,30} = 11.133$	≤0.001[b]	0.341	0.988
NOR ratio	0.005[b]	0.048[a]	0.483	$F_{2,30} = 4.852$	0.013[a]	0.184	0.773
NOR in the PS Group							
New object time (s)	≤0.001[b]	≤0.001[b]	0.655	$F_{2,30} = 13.367$	≤0.001[b]	0.305	0.997
Old object time (s)	0.001[b]	0.004[b]	0.752	$F_{2,30} = 8.298$	0.001[b]	0.214	0.954
NOR ratio	0.835	0.665	0.839	$F_{2,30} = 0.101$	0.904	0.003	0.065
EPM in the CG							
Open arm time (s)	0.083	0.387	0.455	$F_{2,30} = 1.601$	0.213	0.068	0.321
Closed arm time (s)	≤0.001[b]	≤0.001[b]	0.002[b]	$F_{2,30} = 52.846$	≤0.001[b]	0.706	1.000
Open arm entries	0.266	0.915	0.378	$F_{2,30} = 0.696$	0.504	0.031	0.160
EPM ratio	0.003[b]	0.510	0.041	$F_{2,30} = 4.953$	0.011[a]	0.184	0.783
EPM in the PS Group							
Open arm time (s)	0.003[b]	0.047[a]	0.367	$F_{2,30} = 7.292$	0.002[b]	0.198	0.918
Closed arm time (s)	≤0.001[b]	≤0.001[b]	0.149	$F_{2,30} = 21.709$	≤0.001[b]	0.416	1.000
Open arm entries	≤0.001[b]	0.004[b]	0.173	$F_{2,30} = 13.459$	≤0.001[b]	0.306	0.997
EPM ratio	≤0.001[b]	0.038[a]	0.134	$F_{2,30} = 8.958$	≤0.001[b]	0.227	0.967
Rotarod in the CG							
8 rpm speed (s)	0.090	≤0.001[b]	0.015[a]	$F_{2,30} = 9.737$	≤0.001[b]	0.307	0.976
16 rpm speed (s)	0.148	0.008[b]	0.216	$F_{2,30} = 3.937$	0.027[a]	0.152	0.678
Rotarod in the PS Group							
8 rpm speed (s)	0.494	0.040[a]	0.022[a]	$F_{2,30} = 3.082$	0.053	0.092	0.574
16 rpm speed (s)	0.389	0.347	0.136	$F_{2,30} = 1.144$	0.325	0.036	0.243
BBT in the CG							
Latency (s)	0.417	0.990	0.470	$F_{2,30} = 0.397$	0.675	0.182	0.110
Number of foot slips	0.027[a]	0.111	0.614	$F_{2,30} = 2.948$	0.063	0.118	0.545
BBT in the PS Group							
Latency (s)	0.001[b]	≤0.001[b]	0.254	$F_{2,30} = 12.826$	≤0.001[b]	0.296	0.996
Number of foot slips	≤0.001[b]	≤0.001[b]	0.002[b]	$F_{2,30} = 37.491$	≤0.001[b]	0.551	1.000
MWT in the CG							
Male							
Latency (s)	≤0.001[b]	≤0.001[b]	0.816	$F_{2,126} = 19.718$	≤0.001[b]	0.041	1.000
Distance traveled (m)	≤0.001[b]	≤0.001[b]	0.389	$F_{2,126} = 17.176$	≤0.001[b]	0.035	1.000
Probe time (%)	0.783	0.709	0.912	$F_{2,30} = 0.083$	0.921	0.006	0.061
Female							
Latency (s)	0.080	0.014[a]	0.406	$F_{2,126} = 3.572$	0.029[a]	0.009	0.663
Distance traveled (m)	0.097	0.003[b]	0.182	$F_{2,126} = 4.647$	0.010[a]	0.012	0.783
Probe time (%)	0.809	0.689	0.870	$F_{2,30} = 0.085$	0.919	0.009	0.061
MWT in the PS Group							
Male							
Latency (s)	0.001[b]	0.061	0.478	$F_{2,126} = 5.991$	0.003[b]	0.015	0.881
Distance traveled (m)	0.017[a]	0.176	0.624	$F_{2,126} = 3.052$	0.048[a]	6.104	0.590
Probe time (%)	0.358	0.160	0.588	$F_{2,30} = 1.128$	0.340	0.083	0.226
Female							
Latency (s)	0.522	0.197	0.459	$F_{2,126} = 0.862$	0.423	0.002	0.199
Distance traveled (m)	0.344	0.230	0.669	$F_{2,126} = 0.895$	0.409	0.002	0.205
Probe time (%)	0.014[a]	0.006[b]	0.388	$F_{2,30} = 6.255$	0.005[b]	0.263	0.868

Key: BBT, balance beam test; CG, control group; dfd (N-G), degrees of freedom denominator; dfn (G-1), degrees of freedom numerator; EPM, elevated plus maze; MWT, Morris water task; NOR, novel object recognition; Partial η^2, an estimate of effect size; PS, prenatal stress.
Repeated measures ANOVAs were used for statistical analyses.
[a] $p < 0.05$.
[b] $p < 0.01$.
[c] The "between groups' *p*-values" show *p*-values for the between-group comparisons.
[d] The "significant main effects" indicate the statistical results of a significant main effect for every measure.

was also significantly higher in the female CG than the male CG in A4 and A6 total PA and in HB at 6 months (Fig. S2, Table 5). Increase in Aβ accumulation throughout age was significant in all groups (Table 6).

The largest Aβ plaque size (μm) was also significantly larger in the PS groups than the CG at 2, 4, 6, and 10 months except in section A6 at 2 months (Table 5). The sex effect was observed in sections A3, A4, and A6 at 6 months and sections A2 and A4 at 10 months for the PS group (Fig. 5, Table 5).

3.4. The interaction of the age and PS on results

The interaction effect was significant for the PPI amplitude, NOR ratio, elevated plus maze measures, balance beam test measures, latency of the MWT ($p = 0.004$), total PA of the A4, A5, and A6, PA in OA, ACA, NA, HR, RA, EA, CAA, MB, and HB, and plaque size of A1-A5 (Table 7). The findings indicated that independent of the effects of either the PS or age on results, some measures also influenced from the interaction of the age and PS.

Table 3
Comparing the PS and control groups in different measures of the behavioral tests

Behavioural Tests	Significant main effects[c]			
	$F_{dfn,dfd}$	p	η^2	Power
PPI of the ASR Test				
ASR amplitude (%) at 1 mo	$F_{1,158} = 0.007$	0.934	0.000	0.051
ASR amplitude (%) at 2 mo	$F_{1,126} = 0.097$	0.757	0.002	0.061
ASR amplitude (%) at 4 mo	$F_{1,94} = 0.752$	0.391	0.019	0.135
ASR amplitude (%) at 6 mo	$F_{1,66} = 0.201$	0.289	0.061	0.279
ASR amplitude (%) at 10 mo	$F_{1,30} = 0.790$	0.381	0.026	0.138
PPI amplitude (%) at 1 mo	$F_{1,158} = 0.081$	0.777	0.001	0.059
PPI amplitude (%) at 2 mo	$F_{1,126} = 10.695$	0.002[b]	0.201	0.892
PPI amplitude (%) at 4 mo	$F_{1,94} = 10.879$	0.002[b]	0.219	0.910
PPI amplitude (%) at 6 mo	$F_{1,66} = 8.222$	0.007[b]	0.210	0.803
PPI amplitude (%) at 10 mo	$F_{1,30} = 9.096$	0.005[b]	0.233	0.831
ASR latency (ms) at 1 mo	$F_{1,158} = 0.092$	0.763	0.092	0.060
ASR latency (ms) at 2 mo	$F_{1,126} = 0.874$	0.324	0.102	0.187
ASR latency (ms) at 4 mo	$F_{1,94} = 0.092$	0.763	0.092	0.060
ASR latency (ms) at 6 mo	$F_{1,66} = 0.609$	0.280	0.018	0.118
ASR latency (ms) at 10 mo	$F_{1,30} = 0.017$	0.898	0.001	0.052
PPI latency (ms) at 1 mo	$F_{1,158} = 1.459$	0.231	0.020	0.222
PPI latency (ms) at 2 mo	$F_{1,126} = 9.535$	0.004[b]	0.192	0.845
PPI latency (ms) at 4 mo	$F_{1,94} = 0.628$	0.432	0.015	0.121
PPI latency (ms) at 6 mo	$F_{1,66} = 10.017$	0.006[b]	0.371	0.857
PPI latency (ms) at 10 mo	$F_{1,30} = 9.316$	0.009[a]	0.365	0.704
NOR Test				
Initial exploration time (s) at 2 mo	$F_{1,126} = 0.671$	0.404	0.092	0.127
Initial exploration time (s) at 6 mo	$F_{1,66} = 0.102$	0.752	0.081	0.071
Initial exploration time (s) at 10 mo	$F_{1,30} = 0.503$	0.301	0.058	0.098
New object time (s) at 2 mo	$F_{1,126} = 4.319$	0.042[a]	0.074	0.532
New object time (s) at 6 mo	$F_{1,66} = 19.88$	≤0.001[b]	0.432	0.992
New object time (s) at 10 mo	$F_{1,30} = 15.648$	0.001[b]	0.405	0.996
Old object time (s) at 2 mo	$F_{1,126} = 1.300$	0.259	0.024	0.201
Old object time (s) at 6 mo	$F_{1,66} = 2.567$	0.121	0.087	0.339
Old object time (s) at 10 mo	$F_{1,30} = 4.587$	0.037[a]	0.186	0.553
NOR ratio at 2 mo	$F_{1,126} = 4.755$	0.040[a]	0.091	0.587
NOR ratio at 6 mo	$F_{1,66} = 18.537$	≤0.001[b]	0.407	0.986
NOR ratio at 10 mo	$F_{1,30} = 8.339$	0.008[b]	0.266	0.790
EPM Test				
Open arm time (s) at 2 mo	$F_{1,126} = 0.814$	0.371	0.015	0.144
Open arm time (s) at 6 mo	$F_{1,66} = 34.628$	≤0.001[b]	0.562	1.000
Open arm time (s) at 10 mo	$F_{1,30} = 21.164$	≤0.001[b]	0.457	0.982
Closed arm time (s) at 2 mo	$F_{1,126} = 1.499$	0.226	0.027	0.225
Closed arm time (s) at 6 mo	$F_{1,66} = 83.861$	≤0.001[b]	0.765	1.000
Closed arm time (s) at 10 mo	$F_{1,30} = 77.731$	≤0.001[b]	0.724	1.000
Number of entries to open arm at 2 mo	$F_{1,126} = 0.175$	0.678	0.003	0.070
Number of entries to open arm at 6 mo	$F_{1,66} = 43.683$	≤0.001[b]	0.618	1.000
Number of entries to open arm at 10 mo	$F_{1,30} = 11.442$	0.003[b]	0.332	0.899
EPM ratio at 2 mo	$F_{1,126} = 0.024$	0.877	0.001	0.053
EPM ratio at 6 mo	$F_{1,66} = 48.902$	≤0.001[b]	0.644	1.000
EPM ratio at 10 mo	$F_{1,30} = 9.533$	0.005[b]	0.301	0.867
Rotarod Test				
8 rpm speed (s) at 2 mo	$F_{1,126} = 0.211$	0.648	0.004	0.074
8 rpm speed (s) at 6 mo	$F_{1,66} = 4.665$	0.046[a]	0.220	0.555
8 rpm speed (s) at 10 mo	$F_{1,30} = 4.791$	0.044[a]	0.192	0.532
16 rpm speed (s) at 2 mo	$F_{1,126} = 0.079$	0.780	0.049	0.059
16 rpm speed (s) at 6 mo	$F_{1,66} = 7.059$	0.013[a]	0.207	0.726
16 rpm speed (s) at 10 mo	$F_{1,30} = 4.771$	0.043[a]	0.221	0.501
BBT				
Latency (s) at 2 mo	$F_{1,126} = 0.024$	0.876	0.001	0.053
Latency (s) at 6 mo	$F_{1,66} = 20.832$	≤0.001[b]	0.432	0.993
Latency (s) at 10 mo	$F_{1,30} = 10.504$	0.005[b]	0.412	0.857
Foot slips at 2 mo	$F_{1,126} = 0.218$	0.642	0.004	0.074
Foot slips at 6 mo	$F_{1,66} = 41.501$	≤0.001[b]	0.606	1.000
Foot slips at 10 mo	$F_{1,30} = 111.91$	≤0.001[b]	0.882	1.000

Key: ANOVA, analysis of variance; BBT, balance beam test; dfd (N-G), degrees of freedom denominator; dfn (G-1), degrees of freedom numerator; EPM, elevated plus maze; NOR, novel object recognition; PPI of the ASR, prepulse inhibition of the acoustic startle reflex; Partial η^2, an estimate of effect size; PS, prenatal stress.
Univariate ANOVAs were used for statistical analyses.
[a] $p < 0.05$.
[b] $p < 0.01$.
[c] The "between groups' p-values" show p-values for the between-group comparisons.

4. Discussion

The 5 main findings were (1) The PS resulted in dysregulation of the HPA axis in both sexes, which was stronger in females and was not modified by age; (2) the PS offspring exhibited impairments in all cognitive and motor tasks compared with the CG; (3) the PS accelerated the onset age of showing a significant Aβ pathology by 2–3 months; (4) The PS induced a significant overproduction of the

Table 4
Statistical results of comparing the repeat of the PPI of the ASR across age per group

The ASR of the PPI Test	Between groups' *p*-Values[c]										Significant main effects[d]			
	1, 2 mo	1, 4 mo	1, 6 mo	1, 10 mo	2, 4 mo	2, 6 mo	2, 10 mo	4, 6 mo	4, 10 mo	6, 10 mo	$F_{dfn,dfd}$	*p*	η^2	Power
Control Group														
ASR amplitude (%)	0.167	0.379	0.014[a]	0.003[b]	0.063	0.001[b]	≤0.001[b]	0.176	0.045[a]	0.46	$F_{4,48} = 5.15$	0.001[b]	0.158	0.962
PPI amplitude (%)	≤0.001[b]	≤0.001[b]	≤0.001[b]	≤0.001[b]	0.008[b]	0.175	0.444	0.239	0.141	0.240	$F_{4,48} = 23.87$	≤0.001[b]	0.465	1.000
ASR latency (ms)	0.410	0.589	0.001[b]	≤0.001[b]	0.250	0.001[b]	≤0.001[b]	0.020[a]	0.002[b]	0.312	$F_{4,48} = 7.27$	≤0.001[b]	0.206	0.995
PPI latency (ms)	0.524	≤0.001[b]	≤0.001[b]	0.024[b]	0.004[b]	≤0.001[b]	0.097	0.070	0.463	0.026[a]	$F_{4,48} = 11.30$	≤0.001[b]	0.289	1.000
PS Group														
ASR amplitude (%)	0.501	0.065	0.013[a]	≤0.001[b]	0.020[a]	0.004[b]	≤0.001[b]	0.389	0.042[a]	0.314	$F_{4,48} = 6.38$	≤0.001[b]	0.200	0.988
PPI amplitude (%)	0.425	0.001	0.021[a]	0.156	0.015[a]	0.130	0.555	0.489	0.068	0.339	$F_{4,48} = 3.59$	0.009[b]	0.120	0.859
ASR latency (ms)	0.232	0.267	≤0.001[b]	0.001[b]	0.261	0.048[a]	0.010[a]	0.003[b]	0.015[a]	0.485	$F_{4,48} = 6.90$	≤0.001[b]	0.230	0.987
PPI latency (ms)	0.052	0.006[b]	≤0.001[b]	≤0.001[b]	0.524	0.003[b]	0.047[a]	0.011[a]	0.137	0.279	$F_{4,48} = 8.02$	≤0.001[b]	0.241	0.998

Key: ANOVA, analysis of variance; ASR, acoustic startle reflex; dfd (N-G), degrees of freedom denominator; dfn (G-1), degrees of freedom numerator; Partial η^2, an estimate of effect size; PPI, prepulse inhibition; PS, prenatal stress.
Repeated measures ANOVAs were used for statistical analyses.
[a] $p < 0.05$.
[b] $p < 0.01$.
[c] The "between groups' *p*-values" show *p*-values for the between-group comparisons.
[d] The "significant main effects" demonstrate the statistical results of a significant main effect for every measure.

Aβ plaques and also larger plaque size across age; and (5) a sex effect that may account for the higher vulnerability of females than males for developing the AD-like pathology was observed in the HPA axis responsivity, learning ability, and Aβ aggregation, especially in the PS group. We consider these findings in turn.

4.1. The PS created a persistent HPA axis hyperactivity across age

We measured corticosterone levels at 3 time spots across age, namely at 2, 6, and 10 months. The PS resulted in a higher HPA axis responsivity at 2 months, which was more hyperactive in females than males. This pattern of response was replicated at older ages, whereas all groups exhibited a small age effect that was not significant. Current evidence implies that dysregulation of the maternal and fetal HPA axes, and the placenta by the PS, are the most likely candidates for these alternations (Charil et al., 2010; Huizink et al., 2004; Jafari et al., 2018b; Weinstock, 2017). It has been shown that PS is associated with a higher basal glucocorticoid secretion (Fameli et al., 1994; Jafari et al., 2017d; Maccari et al., 1995; Ward et al., 2000; Weinstock et al., 1992), and a slower recovery after stress (Fride et al., 1986; Jafari et al., 2017d; Maccari et al., 1995; Uno et al., 1994) especially in female rats (Weinstock et al., 1992). The PS also affects hippocampal GRs involved in the negative feedback loop that inhibits the hormonal stress response and restores the system to a constant state (Charil et al., 2010). The reduction in the density of hippocampal GRs in the PS offspring (Henry et al., 1994; Szuran et al., 2000; Weinstock et al., 1992) has also been female specific in some studies (Szuran et al., 2000; Weinstock et al., 1992).

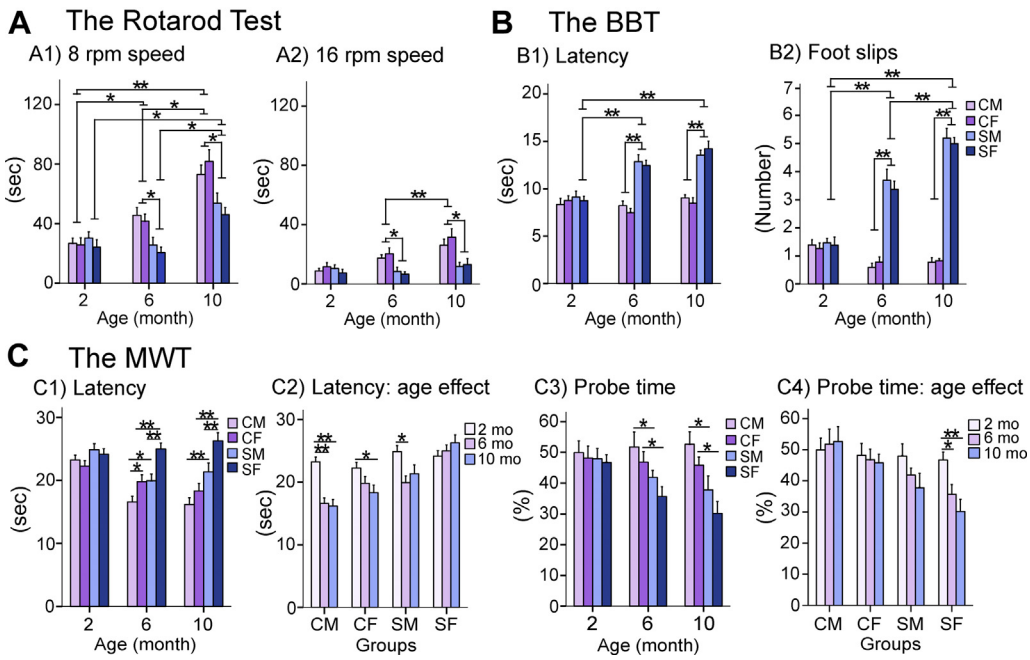

Fig. 3. Results of behavioral tests. (A) The rotarod test: (A1 and A2) A shorter rotarod time (sec) in the PS group compared with the control group. The rotarod time improvement by age was only observed in the CG. (B) The BBT: (B1 and B2) The PS group displayed a significantly longer latency (sec) and a higher number of foot slips compared with the CG at higher ages. Impaired results by age only were shown in the PS group. (C) The MWT: (C1) The swim latency (sec) was significantly higher in females than males at 6 months for the CG and at 6 and 10 months for the PS group. The latency was also significantly higher in the PS group compared with the CG at higher ages. (C2) Improvement by age was not shown in the SF group; that is, CM > CF > SM > SF. (C3) The probe test: The same pattern of lower scores in the PS group than the CG was observed, that is, SF < SM < CF < CM. A significantly impaired probe time by age only was shown in SF group. Results reported as mean ± SEM. Asterisks indicate $^*p < 0.05$ or $^{**}p < 0.01$. Abbreviations: BBT, balance beam test; CF, control female; CG, control group; CM, control male; MWT, Morris water task; PS, prenatal stress; SF, stress female; SM, stress male.

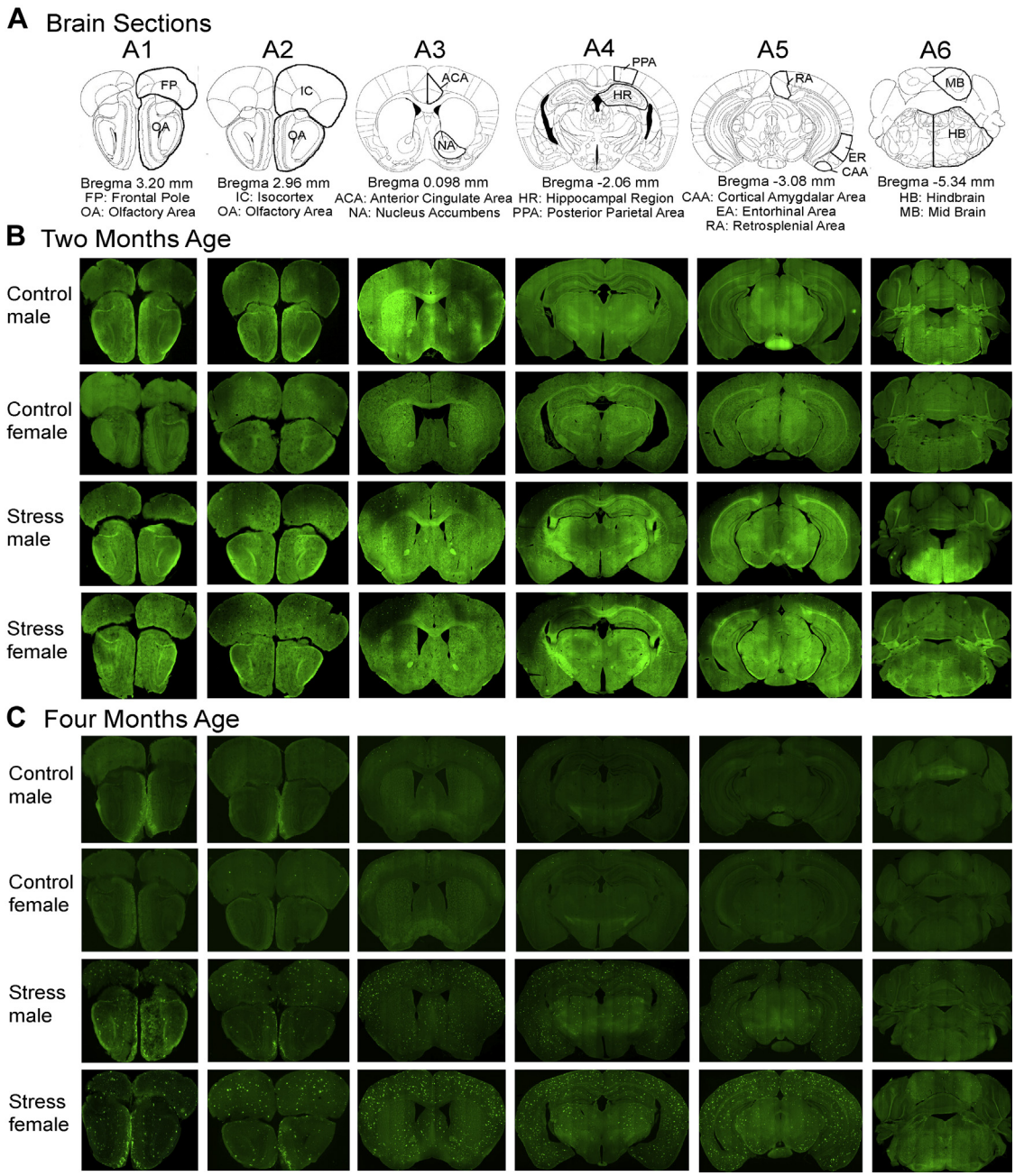

Fig. 4. The Aβ plaque area at 2 and 4 months. (A) Six coronal sections (A1-A6) selected for quantifying the Aβ plaque area (%) in the 4 groups. (B) Samples of 6 coronal sections at 2 months: Except for the section A6 that was clear of any Aβ plaques, the PS groups displayed a significantly higher PA and larger plaque size (μm) in all sections relative to the CGs. The PA was also significantly higher in most of the specific brain areas underlined (refer to Fig. 5 for details of statistical analyses). (C) Samples of 6 coronal sections at 4 months: PS groups exhibited a significantly higher PA and larger plaque size (μm) in all sections and specific brain regions compared with the CGs (refer to Fig. 5). Abbreviations: Aβ, amyloid beta; CG, control group; OA, olfactory area; PS, prenatal stress.

During pregnancy, CRH was synthesized by the placenta and released into the maternal and fetal blood flow. This placental CRH activity is modulated by the maternal HPA axis (Huizink et al., 2004). The PS activates the maternal HPA axis, resulting in excess production and release of placental CRH into the bloodstream that influences the hippocampus function and integrity (Sandman et al., 2006) and also other parahippocampal and limbic areas rich in CRH receptors that are involved in mood disorders, anxiety, aggression, and impulsivity disorders (Wadhwa et al., 2004). In addition, the PS adversely affects functions of the placenta such as delivering nutrients and oxygen to the fetus via altering placental morphology and growth (Angiolini et al., 2006) and reducing the blood flow by increasing vascular resistance (Charil et al., 2010). The PS also increases proinflammatory cytokines in placental tissues, which have been found to be associated with neurodevelopmental disorders (Crocker, 2006).

Beyond the HPA axis, the sympathetic-adrenal-medullary system is another neuroendocrine system known to be highly susceptible to the influence of gestational and environmental factors during development (Young, 2002). Various studies have implicated that the PS may lead to a significant increase in catecholamines levels, that is, norepinephrine and epinephrine, resulting in placental hypoperfusion and subsequent constraints of oxygen and nutrients to the fetus, leading to fetal growth impairments (de Weerth and Buitelaar, 2005; Su et al., 2015).

Table 5
Comparing the PS and control groups in Aβ quantifications (plaque area and plaque size) across age

Plaque area (%) and plaque size (μm)	Between groups' *p*-Values[c]				Significant main effects[d]			
	CM, SM	CF, SF	CM, CF	SM, SF	$F_{dfn,dfd}$	*p*	η^2	Power
2 mo								
A1 total plaque area (%)	≤0.001[b]	≤0.001[b]	0.435	0.387	$F_{3,124} = 18.186$	≤0.001[b]	0.694	1.000
FP (%)	≤0.001[b]	≤0.001[b]	0.134	0.657	$F_{3,124} = 40.621$	≤0.001[b]	0.835	1.000
OA (%)	0.007[b]	≤0.001[b]	0.437	0.201	$F_{3,124} = 7.586$	0.001[b]	0.487	0.970
Size (μm)	0.009[a]	0.006[b]	0.684	0.428	$F_{3,124} = 5.969$	0.004[b]	0.438	0.918
A2 total plaque area (%)	0.006[b]	0.002[b]	0.804	0.444	$F_{3,124} = 7.264$	0.001[b]	0.476	0.963
IC (%)	≤0.001[b]	≤0.001[b]	0.452	0.346	$F_{3,124} = 24.451$	≤0.001[b]	0.753	1.000
Size (μm)	0.003[b]	0.002[b]	0.845	0.703	$F_{3,124} = 7.747$	0.001[b]	0.514	0.971
A3 total plaque area (%)	0.005[b]	0.088	0.579	0.457	$F_{3,124} = 4.269$	0.015[a]	0.348	0.799
ACA (%)	0.036[a]	0.012[a]	0.890	0.546	$F_{3,124} = 4.178$	0.016[a]	0.343	0.789
NA (%)	0.213	0.243	0.656	0.416	$F_{3,124} = 1.228$	0.321	0.133	0.286
Size (μm)	≤0.001[b]	≤0.001[b]	0.498	0.661	$F_{3,124} = 14.228$	≤0.001[b]	0.640	1.000
A4 total plaque area (%)	0.006[b]	0.002[b]	0.804	0.441	$F_{3,124} = 7.264$	0.001[b]	0.476	0.963
PPA (%)	0.007[b]	≤0.001[b]	0.839	0.382	$F_{3,124} = 7.472$	0.001[b]	0.483	0.968
HR (%)	0.228	0.065	0.833	0.179	$F_{3,124} = 1.920$	0.153	0.194	0.433
Size (μm)	0.018[a]	0.012[a]	0.637	0.483	$F_{3,124} = 4.888$	0.009[b]	0.400	0.849
A5 total plaque area (%)	0.015[a]	0.040[a]	0.416	0.707	$F_{3,124} = 4.102$	0.017[a]	0.339	0.781
RA (%)	0.034[a]	0.014[a]	0.939	0.645	$F_{3,124} = 4.072$	0.018[a]	0.337	0.778
EA (%)	0.149	0.243	0.245	0.380	$F_{3,124} = 1.941$	0.150	0.195	0.437
CAA (%)	0.104	0.058	0.694	0.493	$F_{3,124} = 2.470$	0.086	0.236	0.540
Size (μm)	0.018[a]	0.032[a]	0.679	0.877	$F_{3,124} = 3.992$	0.021[a]	0.353	0.762
4 mo								
A1 total plaque area (%)	≤0.001[b]	≤0.001[b]	0.871	0.363	$F_{3,92} = 12.142$	≤0.001[b]	0.603	0.999
FP (%)	0.026[a]	0.004[b]	0.962	0.389	$F_{3,92} = 5.466$	0.005[b]	0.406	0.894
OA (%)	0.003[b]	0.010[a]	0.229	0.465	$F_{3,92} = 6.869$	0.002[b]	0.462	0.953
Size (μm)	0.002[b]	0.002[b]	0.921	0.608	$F_{3,92} = 9.068$	≤0.001[b]	0.531	0.988
A2 total plaque area (%)	≤0.001[b]	≤0.001[b]	0.466	0.865	$F_{3,92} = 18.849$	≤0.001[b]	0.702	1.000
IC (%)	≤0.001[b]	≤0.001[b]	0.790	0.507	$F_{3,92} = 23.174$	≤0.001[b]	0.743	1.000
Size (μm)	≤0.001[b]	≤0.001[b]	0.750	0.253	$F_{3,92} = 21.303$	≤0.001[b]	0.727	1.000
A3 total plaque area (%)	≤0.001[b]	≤0.001[b]	0.447	0.479	$F_{3,92} = 18.391$	≤0.001[b]	0.697	1.000
ACA (%)	0.001[b]	0.001[b]	0.828	0.587	$F_{3,92} = 10.016$	≤0.001[b]	0.556	0.994
NA (%)	≤0.001[b]	≤0.001[b]	0.664	0.738	$F_{3,92} = 14.339$	≤0.001[b]	0.642	1.000
Size (μm)	0.001[b]	0.001[b]	0.793	0.551	$F_{3,92} = 11.773$	≤0.001[b]	0.595	0.998
A4 total plaque area (%)	≤0.001[b]	≤0.001[b]	0.837	0.906	$F_{3,92} = 13.871$	≤0.001[b]	0.634	1.000
PPA (%)	≤0.001[b]	0.002[b]	0.261	0.877	$F_{3,92} = 11.415$	≤0.001[b]	0.588	0.908
HR (%)	≤0.001[b]	≤0.001[b]	0.709	0.812	$F_{3,92} = 35.095$	≤0.001[b]	0.814	1.000
Size (μm)	≤0.001[b]	≤0.001[b]	0.655	0.722	$F_{3,92} = 23.223$	≤0.001[b]	0.744	1.000
A5 total plaque area (%)	≤0.001[b]	≤0.001[b]	0.801	0.699	$F_{3,92} = 13.962$	≤0.001[b]	0.636	1.000
RA (%)	≤0.001[b]	≤0.001[b]	0.530	0.607	$F_{3,92} = 16.408$	≤0.001[b]	0.672	1.000
EA (%)	≤0.001[b]	≤0.001[b]	0.424	0.738	$F_{3,92} = 32.388$	≤0.001[b]	0.802	1.000
CAA (%)	≤0.001[b]	≤0.001[b]	0.664	0.804	$F_{3,92} = 22.162$	≤0.001[b]	0.735	1.000
Size (μm)	≤0.001[b]	0.002[b]	0.683	0.674	$F_{3,92} = 9.781$	≤0.001[b]	0.550	0.993
A6 total plaque area (%)	≤0.001[b]	≤0.001[b]	0.728	0.377	$F_{3,92} = 12.892$	≤0.001[b]	0.617	0.999
MB (%)	≤0.001[b]	≤0.001[b]	0.864	0.648	$F_{3,92} = 23.766$	≤0.001[b]	0.748	1.000
HB (%)	0.005[b]	0.003[b]	0.657	0.506	$F_{3,92} = 7.178$	0.001[b]	0.473	0.961
Size (μm)	≤0.001[b]	≤0.001[b]	0.504	0.607	$F_{3,92} = 17.658$	≤0.001[b]	0.688	1.000
6 mo								
A1 total plaque area (%)	≤0.001[b]	≤0.001[b]	0.225	0.025[a]	$F_{3,64} = 17.093$	≤0.001[b]	0.681	1.000
FP (%)	0.005[b]	≤0.001[b]	0.411	0.041[a]	$F_{3,64} = 10.565$	≤0.001[b]	0.569	0.996
OA (%)	≤0.001[b]	≤0.001[b]	0.281	0.429	$F_{3,64} = 14.584$	≤0.001[b]	0.646	1.000
Size (μm)	≤0.001[b]	≤0.001[b]	0.414	0.173	$F_{3,64} = 29.449$	≤0.001[b]	0.786	1.000
A2 total plaque area (%)	0.008[a]	0.001[b]	0.586	0.044[a]	$F_{3,64} = 8.111$	0.001[b]	0.503	0.978
IC (%)	0.002[b]	≤0.001[b]	0.148	0.028[a]	$F_{3,64} = 13.190$	≤0.001[b]	0.622	0.999
Size (μm)	≤0.001[b]	≤0.001[b]	0.208	0.240	$F_{3,64} = 16.616$	≤0.001[b]	0.675	1.000
A3 total plaque area (%)	≤0.001[b]	≤0.001[b]	0.216	0.013[a]	$F_{3,64} = 20.544$	≤0.001[b]	0.720	1.000
ACA (%)	0.004[b]	≤0.001[b]	0.370	0.046[a]	$F_{3,64} = 10.949$	≤0.001[b]	0.599	0.997
NA (%)	0.009[b]	0.003[b]	0.394	0.183	$F_{3,64} = 7.163$	0.001[b]	0.472	0.961
Size (μm)	0.001[b]	≤0.001[b]	0.865	0.031[a]	$F_{3,64} = 19.420$	≤0.001[b]	0.708	1.000
A4 total plaque area (%)	≤0.001[b]	≤0.001[b]	0.024[a]	0.031[a]	$F_{3,64} = 18.902$	≤0.001[b]	0.703	1.000
PPA (%)	0.021[a]	0.007[b]	0.513	0.266	$F_{3,64} = 5.462$	0.005[b]	0.406	0.894
HR (%)	≤0.001[b]	≤0.001[b]	0.156	0.190	$F_{3,64} = 16.117$	≤0.001[b]	0.668	1.000
Size (μm)	≤0.001[b]	≤0.001[b]	0.745	0.006[b]	$F_{3,64} = 19.450$	≤0.001[b]	0.709	1.000
A5 total plaque area (%)	≤0.001[b]	≤0.001[b]	0.525	0.018[a]	$F_{3,64} = 13.454$	≤0.001[b]	0.627	0.999
RA (%)	≤0.001[b]	≤0.001[b]	0.193	0.046[a]	$F_{3,64} = 15.194$	≤0.001[b]	0.655	1.000
EA (%)	≤0.001[b]	≤0.001[b]	0.277	0.206	$F_{3,64} = 12.653$	≤0.001[b]	0.613	0.999
CAA (%)	≤0.001[b]	≤0.001[b]	0.173	0.136	$F_{3,64} = 13.672$	≤0.001[b]	0.631	1.000
Size (μm)	0.001[b]	≤0.001[b]	0.828	0.250	$F_{3,64} = 13.716$	≤0.001[b]	0.634	1.000
A6 total plaque area (%)	≤0.001[b]	≤0.001[b]	0.006[b]	≤0.001[b]	$F_{3,64} = 30.013$	≤0.001[b]	0.790	1.000
MB (%)	≤0.001[b]	≤0.001[b]	0.104	0.172	$F_{3,64} = 15.595$	≤0.001[b]	0.661	1.000
HB (%)	≤0.001[b]	≤0.001[b]	0.016[a]	≤0.001[b]	$F_{3,64} = 27.046$	≤0.001[b]	0.772	1.000
Size (μm)	0.016[a]	≤0.001[b]	0.617	0.020[a]	$F_{3,64} = 10.685$	≤0.001[b]	0.572	0.996

Table 5 (*continued*)

Plaque area (%) and plaque size (μm)	Between groups' *p*-Values[c]				Significant main effects[d]			
	CM, SM	CF, SF	CM, CF	SM, SF	$F_{dfn,dfd}$	*p*	η^2	Power
10 mo								
A1 total plaque area (%)	0.009[b]	0.008[b]	0.744	0.753	$F_{3,28} = 5.295$	0.006[b]	0.398	0.883
FP (%)	0.004[b]	0.034[a]	0.241	0.764	$F_{3,28} = 5.380$	0.006[b]	0.402	0.889
OA (%)	≤0.001[b]	≤0.001[b]	0.559	0.549	$F_{3,28} = 12.033$	≤0.001[b]	0.601	0.999
Size (μm)	≤0.001[b]	≤0.001[b]	0.177	0.251	$F_{3,28} = 27.378$	≤0.001[b]	0.774	1.000
A2 total plaque area (%)	0.008[a]	0.001[b]	0.602	0.704	$F_{3,28} = 12.686$	0.001[b]	0.613	0.999
IC (%)	≤0.001[b]	≤0.001[b]	0.699	0.482	$F_{3,28} = 28.395$	≤0.001[b]	0.780	1.000
Size (μm)	0.001[b]	≤0.001[b]	0.601	0.042[a]	$F_{3,28} = 15.484$	≤0.001[b]	0.679	1.000
A3 total plaque area (%)	0.002[b]	0.004[b]	0.437	0.548	$F_{3,28} = 7.617$	0.001[b]	0.488	0.971
ACA (%)	0.038[a]	0.007[b]	0.651	0.235	$F_{3,28} = 4.974$	0.008[b]	0.383	0.861
NA (%)	0.001[b]	0.001[b]	0.318	0.381	$F_{3,28} = 9.816$	≤0.001[b]	0.551	0.993
Size (μm)	≤0.001[b]	≤0.001[b]	0.467	0.287	$F_{3,28} = 15.773$	≤0.001[b]	0.663	1.000
A4 total plaque area (%)	0.006[b]	0.009[b]	0.028[a]	0.041[a]	$F_{3,28} = 8.838$	≤0.001[b]	0.525	0.987
PPA (%)	0.008[b]	0.003[b]	0.227	0.134	$F_{3,28} = 7.714$	0.001[b]	0.491	0.972
HR (%)	0.004[b]	0.002[b]	0.752	0.0.550	$F_{3,28} = 7.436$	0.001[b]	0.482	0.967
Size (μm)	0.001[b]	≤0.001[b]	0.800	0.036[a]	$F_{3,28} = 28.616$	≤0.001[b]	0.783	1.000
A5 total plaque area (%)	0.005[b]	0.009[b]	0.295	0.447	$F_{3,28} = 6.284$	0.003[b]	0.440	0.934
RA (%)	≤0.001[b]	≤0.001[b]	0.328	0.205	$F_{3,28} = 12.624$	≤0.001[b]	0.612	0.999
EA (%)	0.012[a]	0.015[a]	0.224	0.267	$F_{3,28} = 5.695$	0.004[b]	0.416	0.907
CAA (%)	0.002[b]	0.005[b]	0.329	0.603	$F_{3,28} = 7.858$	0.001[b]	0.496	0.975
Size (μm)	0.003[b]	0.001[b]	0.826	0.477	$F_{3,28} = 8.836$	≤0.001[b]	0.525	0.987
A6 total plaque area (%)	0.001[b]	≤0.001[b]	0.341	0.275	$F_{3,28} = 11.308$	≤0.001[b]	0.586	0.998
MB (%)	0.001[b]	≤0.001[b]	0.651	0.194	$F_{3,28} = 11.873$	≤0.001[b]	0.597	0.999
HB (%)	≤0.001[b]	≤0.001[b]	0.323	0.127	$F_{3,28} = 17.590$	≤0.001[b]	0.687	1.000
Size (μm)	0.048	0.021[a]	0.417	0.203	$F_{3,28} = 4.468$	0.014[a]	0.398	0.798

Key: ANOVA, analysis of variance; ACA, anterior cingulate area; CAA, cortical amygdalar area; CF, control female; CM, control male; dfd (N-G), degrees of freedom denominator; dfn (G-1), degrees of freedom numerator; EA, entorhinal area; FP, frontal pole; HB, hindbrain; HR, hippocampal region; IC, isocortex; MB, midbrain; NA, nucleus accumbens; OA, olfactory area; Partial η^2, an estimate of effect size; PPA, posterior parietal area; PPC, posterior parietal cortex; PS, prenatal stress; RA, retrosplenial area; SF, stress female; SM, stress male. A univariate ANOVA was used for statistical analyses.

[a] $p < 0.05$.

[b] $p < 0.01$.

[c] The "between groups' *p*-values" show *p*-values for the between-group comparisons.

[d] The "significant main effects" indicate the statistical results of a significant main effect for every measure.

4.2. The PS aggravates learning, cognitive, and motor function

Ample evidence of experimental studies indicates that maternal stressors in rodents can replicate some of the behavioral abnormalities observed in humans including deficits in anxiety-like behavior, social interaction, spatial learning and memory (Weinstock, 2017), and adaptation to postnatal stressful conditions (Huizink et al., 2004). In our study, the PS produced significant enduring impairments in all learning, memory, and cognitive tasks. It resulted in a significant loss in the amplitude and latency of the PPI, which is an index of impairment in sensorimotor gating (Rohleder et al., 2016), a decreased tendency to explore the new object, a sign of impaired attention or short-term memory (Weinstock, 2017), a decreased time spent in open arm and lower entries to open arm as an index of anxiety-like behavior (Burgado et al., 2014; Jafari et al., 2017a) and a markedly longer latency and shorter probe time in MWT specially in females, thus supporting a deficit in spatial learning and memory (Cuadrado-Tejedor et al., 2012; Fang et al., 2018; Jafari et al., 2017c). Ample evidence implies that hyperactivity of the HPA axis due to PS can downregulate receptors in the hippocampus, the hypothalamus, and the pituitary or adrenal glands, decrease the sensitivity of the receptors at any of these levels, alter the CRH levels or affinity of plasma binding proteins (Huizink et al., 2004), and lead to modulations in cognitive performance (Kim et al., 2015). Increased release of both CRH and corticosterone has also been shown in females than males in response to various stressful events (Toufexis et al., 2014).

Among brain neurotransmitter systems, studies suggest that the PS leads to an overactive noradrenergic system with increased central norepinephrine turnover (Huizink et al., 2004). The serotonergic system (5-hydroxytryptamine, 5-HT) that is associated with mood disorders, anxiety, aggression, and impulsivity also has been shown to play a role in brain development. A PS-induced increase in fetal brain 5-HT synthesis owing to the HPA-axis hyperactivity has been shown to result in a reduction of 5-HT binding sites in the hippocampus and affect postnatal development and behavior (Charil et al., 2010; Huizink et al., 2004). The cholinergic system is also implicated in learning and memory and may be involved in mood and cognitive disorders. PS has been found to increase hippocampal acetylcholine release, inhibit the influence of cholinergic receptors on the activity of the HPA axis, downregulate hippocampal GRs, and influence the memory and learning abilities of the offspring (Charil et al., 2010; Huizink et al., 2004). PS is also associated with alterations of dopamine receptor systems. The dopaminergic system is involved in the control of locomotion, cognition, and affect (Huizink et al., 2004), and its alternations have been shown to be associated with delayed early motor development (Barlow et al., 1978) and increased fearfulness to stressful situations (Weinstock, 2017). BDNF as a member of the family of neurotrophins that is expressed in the hippocampus and required for proper development and survival of dopaminergic, GABAergic, cholinergic, and serotonergic neurons is also crucial for learning and memory processes (Autry and Monteggia, 2012). PS has been shown to produce a decrease in BDNF mRNA in the frontal cortex and hippocampus of rodents with a reduction in social interaction (Dong et al., 2015), memory (Ratajczak et al., 2015), or increased anxiety-like behavior (Jia et al., 2015).

In our study, the PS also induced impairments in balance and motor coordination that led to less time in RR and higher foot slips and longer time to traverse across the balance beam. Although mouse studies probing motor performance in APP transgenic mice by applying the RR or other tasks did not report major abnormalities (Bellucci et al., 2006; Dineley et al., 2002; Lalonde et al., 2005), existing evidence suggests that stress can modulate motor system

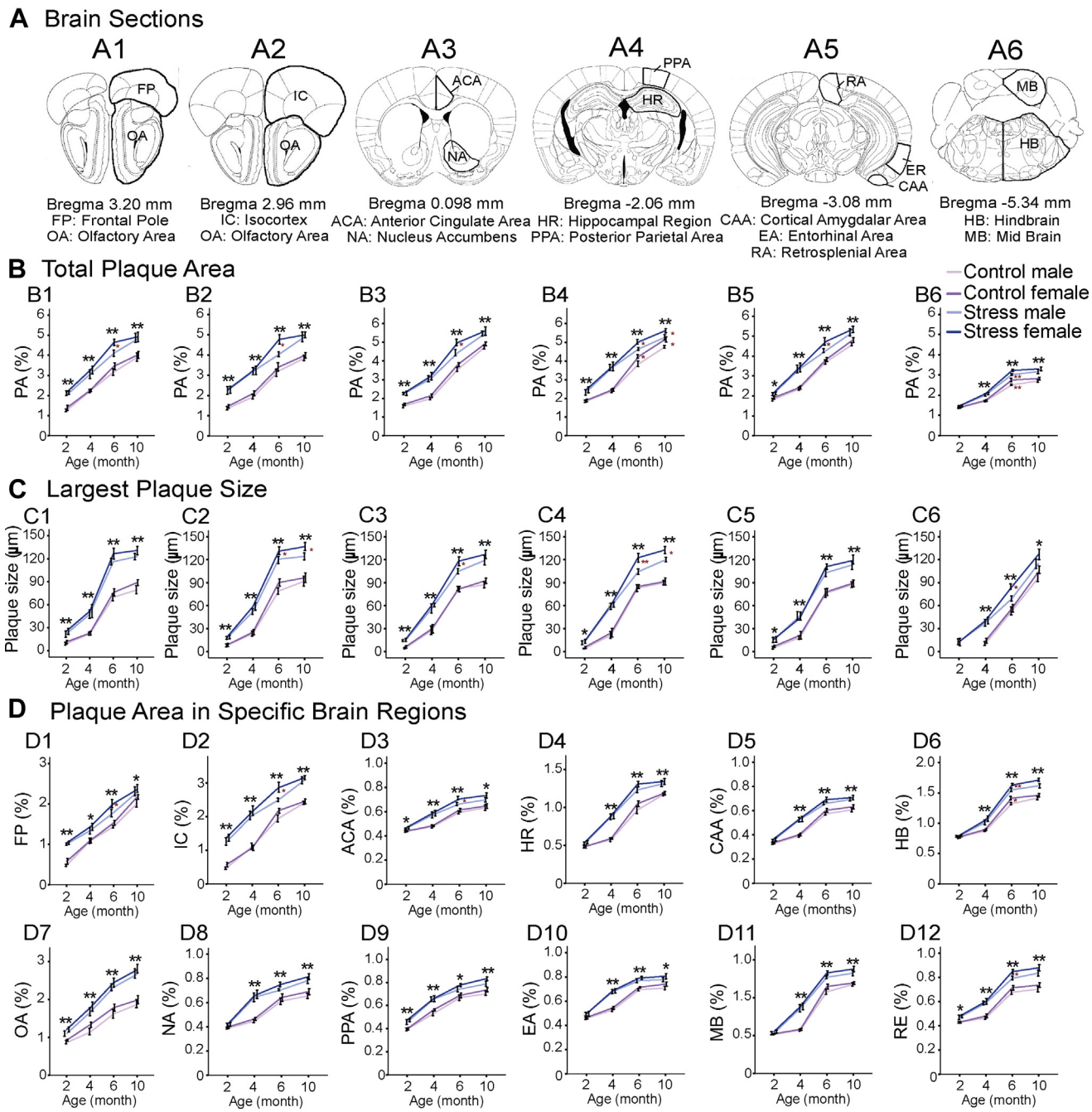

Fig. 5. Development of Aβ aggregation across age. (A) Development of plaque deposition in 6 coronal sections and some specific brain regions underlined was compared between the PS and control groups over age. The plaque area significantly increased by age in all groups (refer to Table 6 for details of statistical analyses). The female mice revealed a significantly higher plaque area and larger plaque size in some measures presented with red asterisks. (B) The total plaque area was significantly higher and (C) the plaque size was significantly larger in the PS groups than the control animals. (D) The plaque area was also significantly larger in all specific brain regions (D1-D12). Black asterisks above each age represent the significant differences between control male and stress male groups as well as control female and stress female groups. Results reported as mean ± SEM. Asterisks indicate $^{*}p < 0.05$ or $^{**}p < 0.01$. Abbreviations: Aβ, amyloid beta; PS, prenatal stress. (For interpretation of the references to color in this figure legend, the reader is referred to the Web version of this article.)

function leading to the pathology of movement disorders (Jafari et al., 2018a,b; Metz, 2007; Metz et al., 2005; Tamura et al., 2012). Although GRs often are found in the limbic system, most parts of the motor system including the motor cortex, cerebellum, basal ganglia (Ahima and Harlan, 1990; Harle et al., 2017), and white matter of the spinal cord (Marlier et al., 1995) also exhibit the presence of GRs leading to be susceptible to the release of stress hormones (Metz, 2007). Extensive evidence implies that hyperactivity of the HPA axis due to stress or glucocorticoid injections can modulate different aspects of balance and motor coordination (Harle et al., 2017; Jafari et al., 2017d, 2018a, 2018b; Metz, 2007; Metz et al., 2005). Neuropathological studies in patients with AD, however, affirm motor disturbances in the later stages of the disease (Suva et al., 1999; Wirths and Bayer, 2008) and also as a characteristic feature of early AD pathology (Scarmeas et al., 2004; Wilson et al., 2000). Thus, the patients with AD manifest a higher level of gait disorder according to the disease stage (Goldman et al., 1999; O'Keeffe et al., 1996). Recent human studies also implicate that PS or anxiety during gestation negatively modifies infant neuromotor development (Grace et al., 2016; van Batenburg-Eddes

Table 6
Statistical results of comparing the repeat of Aβ quantifications (plaque area and plaque size) across age per group

Brain sections	Between groups' p-Values[c]						Significant main effects[d]			
Age	2, 4 mo	2, 6 mo	2, 10 mo	4, 6 mo	4, 10 mo	6, 10 mo	$F_{dfn,dfd}$	p	η^2	Power
Control male										
A1 (%)	≤0.001[b]	≤0.001[b]	≤0.001[b]	≤0.005[b]	≤0.001[b]	0.027[a]	$F_{3,21} = 71.234$	≤0.001[b]	0.922	1.000
IC (%)	≤0.001[b]	≤0.001[b]	≤0.001[b]	0.007[b]	≤0.001[b]	0.002[b]	$F_{3,21} = 135.301$	≤0.001[b]	0.958	1.000
OA (%)	0.086	0.001[b]	≤0.001[b]	0.026[a]	0.002[b]	0.228	$F_{3,21} = 18.592$	≤0.001[b]	0.756	1.000
Size (μm)	0.001[b]	≤0.001[b]	≤0.001[b]	≤0.001[b]	≤0.001[b]	0.233	$F_{3,21} = 84.307$	≤0.001[b]	0.934	1.000
A2 (%)	0.001[b]	0.001[b]	≤0.001[b]	0.003[b]	≤0.001[b]	0.033[a]	$F_{3,21} = 71.123$	≤0.001[b]	0.922	1.000
IC (%)	0.001[b]	≤0.001[b]	≤0.001[b]	0.003[b]	≤0.001[b]	0.004[b]	$F_{3,21} = 109.391$	≤0.001[b]	0.948	1.000
Size (μm)	0.007[b]	≤0.001[b]	≤0.001[b]	≤0.001[b]	0.001[b]	0.253	$F_{3,21} = 77.217$	≤0.001[b]	0.939	1.000
A3 (%)	0.012[a]	≤0.001[b]	≤0.001[b]	≤0.001[b]	≤0.001[b]	≤0.001[b]	$F_{3,21} = 240.184$	≤0.001[b]	0.976	1.000
ACA (%)	0.040[a]	≤0.001[b]	≤0.001[b]	≤0.001[b]	≤0.001[b]	0.071	$F_{3,21} = 53.817$	≤0.001[b]	0.900	1.000
NA (%)	0.026[a]	≤0.001[b]	≤0.001[b]	≤0.001[b]	≤0.001[b]	0.168	$F_{3,21} = 55.709$	≤0.001[b]	0.903	1.000
Size (μm)	0.007[b]	≤0.001[b]	≤0.001[b]	≤0.001[b]	≤0.001[b]	0.324	$F_{3,21} = 134.153$	≤0.001[b]	0.957	1.000
A4 (%)	0.003[b]	≤0.001[b]	≤0.001[b]	≤0.001[b]	≤0.001[b]	0.002[b]	$F_{3,21} = 165.702$	≤0.001[b]	0.956	1.000
PPA (%)	≤0.001[b]	≤0.001[b]	≤0.001[b]	≤0.001[b]	≤0.001[b]	0.216	$F_{3,21} = 102.963$	≤0.001[b]	0.945	1.000
HR (%)	0.014[a]	≤0.001[b]	≤0.001[b]	≤0.001[b]	≤0.001[b]	0.010[a]	$F_{3,21} = 138.363$	≤0.001[b]	0.958	1.000
Size (μm)	0.027[a]	≤0.001[b]	≤0.001[b]	≤0.001[b]	≤0.001[b]	0.435	$F_{3,21} = 160.254$	≤0.001[b]	0.970	1.000
A5 (%)	0.004[b]	≤0.001[b]	≤0.001[b]	≤0.001[b]	≤0.001[b]	0.002[b]	$F_{3,21} = 191.845$	≤0.001[b]	0.970	1.000
RA (%)	0.058	≤0.001[b]	≤0.001[b]	≤0.001[b]	≤0.001[b]	0.353	$F_{3,21} = 108.621$	≤0.001[b]	0.948	1.000
EA (%)	≤0.001[b]	≤0.001[b]	≤0.001[b]	≤0.001[b]	≤0.001[b]	0.489	$F_{3,21} = 158.021$	≤0.001[b]	0.963	1.000
CAA (%)	0.004[b]	≤0.001[b]	≤0.001[b]	≤0.001[b]	≤0.001[b]	0.086	$F_{3,21} = 165.841$	≤0.001[b]	0.965	1.000
Size (μm)	0.016[a]	≤0.001[b]	≤0.001[b]	≤0.001[b]	≤0.001[b]	0.308	$F_{3,21} = 97.737$	≤0.001[b]	0.951	1.000
A6 (%)	≤0.001[b]	≤0.001[b]	≤0.001[b]	≤0.001[b]	≤0.001[b]	0.036[a]	$F_{3,21} = 238.203$	≤0.001[b]	0.975	1.000
MB (%)	0.004[b]	≤0.001[b]	≤0.001[b]	≤0.001[b]	≤0.001[b]	0.002[b]	$F_{3,21} = 308.239$	≤0.001[b]	0.981	1.000
HB (%)	0.003[b]	≤0.001[b]	≤0.001[b]	≤0.001[b]	≤0.001[b]	0.008[b]	$F_{3,21} = 227.596$	≤0.001[b]	0.976	1.000
Size (μm)	≤0.001[b]	≤0.001[b]	≤0.001[b]	≤0.001[b]	≤0.001[b]	≤0.001[b]	$F_{3,21} = 88.262$	≤0.001[b]	0.907	1.000
Control Female										
A1 (%)	0.002[b]	≤0.001[b]	≤0.001[b]	≤0.001[b]	≤0.001[b]	0.009[b]	$F_{3,21} = 81.583$	≤0.001[b]	0.931	1.000
IC (%)	0.001[b]	≤0.001[b]	≤0.001[b]	0.004[b]	≤0.001[b]	0.001[b]	$F_{3,21} = 128.813$	≤0.001[b]	0.955	1.000
OA (%)	0.001[b]	≤0.001[b]	≤0.001[b]	0.009[b]	≤0.001[b]	0.182	$F_{3,21} = 40.343$	≤0.001[b]	0.871	1.000
Size (μm)	0.006[b]	≤0.001[b]	≤0.001[b]	≤0.001[b]	≤0.001[b]	0.155	$F_{3,21} = 106.014$	≤0.001[b]	0.946	1.000
A2 (%)	0.019[a]	≤0.001[b]	≤0.001[b]	0.001[b]	≤0.001[b]	0.055	$F_{3,21} = 60.273$	≤0.001[b]	0.909	1.000
IC (%)	0.002[b]	≤0.001[b]	≤0.001[b]	≤0.001[b]	≤0.001[b]	0.040[a]	$F_{3,21} = 191.834$	≤0.001[b]	0.970	1.000
Size (μm)	0.017[a]	≤0.001[b]	≤0.001[b]	≤0.001[b]	≤0.001[b]	0.985	$F_{3,21} = 96.678$	≤0.001[b]	0.951	1.000
A3 (%)	0.007[b]	≤0.001[b]	≤0.001[b]	≤0.001[b]	≤0.001[b]	0.001[b]	$F_{3,21} = 218.337$	≤0.001[b]	0.973	1.000
ACA (%)	≤0.001[b]	≤0.001[b]	≤0.001[b]	≤0.001[b]	≤0.001[b]	0.201	$F_{3,21} = 62.710$	≤0.001[b]	0.913	1.000
NA (%)	0.002[b]	≤0.001[b]	≤0.001[b]	0.001[b]	≤0.001[b]	0.267	$F_{3,21} = 53.507$	≤0.001[b]	0.899	1.000
Size (μm)	0.009[b]	≤0.001[b]	≤0.001[b]	≤0.001[b]	≤0.001[b]	0.130	$F_{3,21} = 106.370$	≤0.001[b]	0.947	1.000
A4 (%)	0.001[b]	≤0.001[b]	≤0.001[b]	≤0.001[b]	≤0.001[b]	0.002[b]	$F_{3,21} = 290.284$	≤0.001[b]	0.980	1.000
PPA (%)	≤0.001[b]	≤0.001[b]	≤0.001[b]	0.002[b]	0.001[b]	0.056	$F_{3,21} = 85.750$	≤0.001[b]	0.935	1.000
HR (%)	0.001[b]	≤0.001[b]	≤0.001[b]	≤0.001[b]	≤0.001[b]	≤0.029[a]	$F_{3,21} = 230.660$	≤0.001[b]	0.975	1.000
Size (μm)	0.032[a]	≤0.001[b]	≤0.001[b]	0.001[b]	≤0.001[b]	0.384	$F_{3,21} = 77.851$	≤0.001[b]	0.940	1.000
A5 (%)	0.008[b]	≤0.001[b]	≤0.001[b]	≤0.001[b]	≤0.001[b]	0.002[b]	$F_{3,21} = 168.187$	≤0.001[b]	0.966	1.000
RA (%)	0.005[b]	≤0.001[b]	≤0.001[b]	≤0.001[b]	≤0.001[b]	0.495	$F_{3,21} = 78.443$	≤0.001[b]	0.929	1.000
EA (%)	≤0.001[b]	≤0.001[b]	≤0.001[b]	≤0.001[b]	≤0.001[b]	0.253	$F_{3,21} = 154.848$	≤0.001[b]	0.963	1.000
CAA (%)	0.001[b]	≤0.001[b]	≤0.001[b]	≤0.001[b]	≤0.001[b]	0.106	$F_{3,21} = 152.547$	≤0.001[b]	0.962	1.000
Size (μm)	0.031[a]	≤0.001[b]	≤0.001[b]	≤0.001[b]	≤0.001[b]	0.358	$F_{3,21} = 79.829$	≤0.001[b]	0.941	1.000
A6 (%)	≤0.001[b]	≤0.001[b]	≤0.001[b]	≤0.001[b]	≤0.001[b]	0.566	$F_{3,21} = 128.547$	≤0.001[b]	0.955	1.000
MB (%)	0.006[b]	≤0.001[b]	≤0.001[b]	≤0.001[b]	≤0.001[b]	0.280	$F_{3,21} = 310.161$	≤0.001[b]	0.981	1.000
HB (%)	0.003[b]	≤0.001[b]	≤0.001[b]	≤0.001[b]	≤0.001[b]	0.085	$F_{3,21} = 346.210$	≤0.001[b]	0.983	1.000
Size (μm)	≤0.001[b]	≤0.001[b]	≤0.001[b]	≤0.001[b]	≤0.001[b]	≤0.001[b]	$F_{3,21} = 70.927$	≤0.001[b]	0.887	1.000
Stress Male										
A1 (%)	0.011[a]	0.011[a]	≤0.001[b]	≤0.001[b]	≤0.002[b]	≤0.030[a]	$F_{3,21} = 33.453$	≤0.001[b]	0.848	1.000
IC (%)	0.016[a]	0.001[b]	≤0.001[b]	0.007[b]	0.001[b]	0.042[a]	$F_{3,21} = 31.495$	≤0.001[b]	0.840	1.000
OA (%)	0.011[a]	≤0.001[b]	≤0.001[b]	0.002[b]	0.002[b]	0.103	$F_{3,21} = 35.967$	≤0.001[b]	0.857	1.000
Size (μm)	0.004[b]	≤0.001[b]	≤0.001[b]	≤0.001[b]	≤0.001[b]	0.395	$F_{3,21} = 123.601$	≤0.001[b]	0.954	1.000
A2 (%)	0.004[b]	≤0.001[b]	≤0.001[b]	0.008[b]	≤0.001[b]	0.002[b]	$F_{3,21} = 45.194$	≤0.001[b]	0.883	1.000
IC (%)	0.002[b]	≤0.001[b]	≤0.001[b]	0.006[b]	≤0.001[b]	0.005[b]	$F_{3,21} = 53.728$	≤0.001[b]	0.900	1.000
Size (μm)	≤0.001[b]	≤0.001[b]	≤0.001[b]	≤0.001[b]	≤0.001[b]	0.730	$F_{3,21} = 116.361$	≤0.001[b]	0.951	1.000
A3 (%)	0.006[b]	≤0.001[b]	≤0.001[b]	0.002[b]	≤0.001[b]	≤0.001[b]	$F_{3,21} = 272.849$	≤0.001[b]	0.978	1.000
ACA (%)	0.003[b]	≤0.001[b]	≤0.001[b]	0.016[a]	0.019[a]	0.195	$F_{3,21} = 33.487$	≤0.001[b]	0.848	1.000
NA (%)	≤0.001[b]	≤0.001[b]	≤0.001[b]	0.207	0.002[b]	0.051	$F_{3,21} = 48.265$	≤0.001[b]	0.889	1.000
Size (μm)	≤0.001[b]	≤0.001[b]	≤0.001[b]	≤0.001[b]	≤0.001[b]	0.072	$F_{3,21} = 110.913$	≤0.001[b]	0.949	1.000
A4 (%)	≤0.001[b]	≤0.001[b]	≤0.001[b]	0.002[b]	≤0.001[b]	0.001[b]	$F_{3,21} = 103.287$	≤0.001[b]	0.945	1.000
PPA (%)	0.001[b]	≤0.001[b]	≤0.001[b]	0.028[a]	0.002[b]	0.325	$F_{3,21} = 41.694$	≤0.001[b]	0.874	1.000
HR (%)	≤0.001[b]	≤0.001[b]	≤0.001[b]	0.001[b]	≤0.001[b]	0.260	$F_{3,21} = 105.844$	≤0.001[b]	0.946	1.000
Size (μm)	≤0.001[b]	≤0.001[b]	≤0.001[b]	≤0.001[b]	≤0.001[b]	0.014[a]	$F_{3,21} = 216.449$	≤0.001[b]	0.973	1.000
A5 (%)	≤0.001[b]	≤0.001[b]	≤0.001[b]	0.0011[a]	0.001[b]	0.002[b]	$F_{3,21} = 79.933$	≤0.001[b]	0.930	1.000
RA (%)	0.002[b]	≤0.001[b]	≤0.001[b]	≤0.001[b]	≤0.001[b]	0.330	$F_{3,21} = 58.294$	≤0.001[b]	0.907	1.000
EA (%)	≤0.001[b]	≤0.001[b]	≤0.001[b]	≤0.019[a]	≤0.001[b]	0.489	$F_{3,21} = 53.956$	≤0.001[b]	0.900	1.000
CAA (%)	≤0.001[b]	≤0.001[b]	≤0.001[b]	≤0.001[b]	≤0.001[b]	0.145	$F_{3,21} = 111.954$	≤0.001[b]	0.949	1.000
Size (μm)	0.003[b]	≤0.001[b]	≤0.001[b]	0.001[b]	≤0.001[b]	0.130	$F_{3,21} = 89.937$	≤0.001[b]	0.937	1.000
A6 (%)	≤0.001[b]	≤0.001[b]	≤0.001[b]	≤0.001[b]	≤0.001[b]	0.176	$F_{3,21} = 131.788$	≤0.001[b]	0.956	1.000
MB (%)	0.001[b]	≤0.001[b]	≤0.001[b]	≤0.001[b]	≤0.001[b]	0.093	$F_{3,21} = 116.111$	≤0.001[b]	0.951	1.000

(*continued on next page*)

Table 6 (*continued*)

Brain sections	Between groups' *p*-Values[c]						Significant main effects[d]			
Age	2, 4 mo	2, 6 mo	2, 10 mo	4, 6 mo	4, 10 mo	6, 10 mo	$F_{dfn,dfd}$	*p*	η^2	Power
HB (%)	0.001[b]	≤0.001[b]	≤0.001[b]	≤0.001[b]	≤0.001[b]	0.183	$F_{3,21} = 160.191$	≤0.001[b]	0.964	1.000
Size (μm)	0.039[a]	≤0.001[b]	≤0.001[b]	0.002[b]	≤0.001[b]	0.002[b]	$F_{3,21} = 64.864$	≤0.001[b]	0.938	1.000
Stress Female										
A1 (%)	≤0.001[b]	≤0.001[b]	≤0.001[b]	0.002[b]	≤0.001[b]	0.374	$F_{3,21} = 63.519$	≤0.001[b]	0.914	1.000
IC (%)	0.001[b]	≤0.001[b]	≤0.001[b]	≤0.001[b]	≤0.001[b]	0.007[b]	$F_{3,21} = 66.801$	≤0.001[b]	0.918	1.000
OA (%)	0.018[a]	≤0.001[b]	≤0.001[b]	0.024[a]	0.003[b]	0.103	$F_{3,21} = 30.519$	≤0.001[b]	0.836	1.000
Size (μm)	0.058	≤0.001[b]	≤0.001[b]	≤0.001[b]	≤0.001[b]	0.719	$F_{3,21} = 56.350$	≤0.001[b]	0.904	1.000
A2 (%)	0.011[a]	≤0.001[b]	≤0.001[b]	0.007[b]	≤0.001[b]	0.567	$F_{3,21} = 36.636$	≤0.001[b]	0.859	1.000
IC (%)	0.003[b]	≤0.001[b]	≤0.001[b]	0.015[a]	0.001[b]	0.160	$F_{3,21} = 41.673$	≤0.001[b]	0.874	1.000
Size (μm)	≤0.001[b]	≤0.001[b]	≤0.001[b]	0.001[b]	≤0.001[b]	0.574	$F_{3,21} = 85.676$	≤0.001[b]	0.935	1.000
A3 (%)	0.005[b]	≤0.001[b]	≤0.001[b]	≤0.001[b]	≤0.001[b]	0.073	$F_{3,21} = 101.750$	≤0.001[b]	0.944	1.000
ACA (%)	0.002[b]	≤0.001[b]	≤0.001[b]	0.006[b]	≤0.001[b]	0.239	$F_{3,21} = 58.083$	≤0.001[b]	0.906	1.000
NA (%)	0.002[b]	≤0.001[b]	≤0.001[b]	0.091	0.015[a]	0.041[a]	$F_{3,21} = 41.345$	≤0.001[b]	0.873	1.000
Size (μm)	≤0.001[b]	≤0.001[b]	≤0.001[b]	≤0.001[b]	≤0.001[b]	0.389	$F_{3,21} = 116.271$	≤0.001[b]	0.951	1.000
A4 (%)	0.007[b]	≤0.001[b]	≤0.001[b]	0.002[b]	0.001[b]	0.014[a]	$F_{3,21} = 67.946$	≤0.001[b]	0.919	1.000
PPA (%)	0.001[b]	≤0.001[b]	≤0.001[b]	≤0.001[b]	≤0.001[b]	≤0.001[b]	$F_{3,21} = 72.918$	≤0.001[b]	0.924	1.000
HR (%)	≤0.001[b]	≤0.001[b]	≤0.001[b]	0.011[a]	0.001[b]	0.558	$F_{3,21} = 132.320$	≤0.001[b]	0.957	1.000
Size (μm)	≤0.001[b]	≤0.001[b]	≤0.001[b]	≤0.001[b]	≤0.001[b]	0.071	$F_{3,21} = 244.583$	≤0.001[b]	0.876	1.000
A5 (%)	0.003[b]	≤0.001[b]	≤0.001[b]	0.004[b]	≤0.001[b]	0.040[a]	$F_{3,21} = 70.386$	≤0.001[b]	0.921	1.000
RA (%)	0.006[b]	≤0.001[b]	≤0.001[b]	≤0.001[b]	≤0.001[b]	0.256	$F_{3,21} = 87.803$	≤0.001[b]	0.936	1.000
EA (%)	≤0.001[b]	≤0.001[b]	≤0.001[b]	0.004[b]	≤0.001[b]	0.630	$F_{3,21} = 62.361$	≤0.001[b]	0.912	1.000
CAA (%)	0.001[b]	≤0.001[b]	≤0.001[b]	0.001[b]	≤0.001[b]	0.641	$F_{3,21} = 65.089$	≤0.001[b]	0.916	1.000
Size (μm)	≤0.001[b]	≤0.001[b]	≤0.001[b]	≤0.001[b]	≤0.001[b]	0.369	$F_{3,21} = 96.701$	≤0.001[b]	0.942	1.000
A6 (%)	≤0.001[b]	≤0.001[b]	≤0.001[b]	≤0.001[b]	≤0.001[b]	0.476	$F_{3,21} = 299.137$	≤0.001[b]	0.980	1.000
MB (%)	≤0.001[b]	≤0.001[b]	≤0.001[b]	≤0.001[b]	≤0.001[b]	0.255	$F_{3,21} = 164.112$	≤0.001[b]	0.965	1.000
HB (%)	0.002[b]	≤0.001[b]	≤0.001[b]	≤0.001[b]	≤0.001[b]	0.009[b]	$F_{3,21} = 292.018$	≤0.001[b]	0.980	1.000
Size (μm)	0.001[b]	≤0.001[b]	≤0.001[b]	0.002[b]	≤0.001[b]	0.007[b]	$F_{3,21} = 107.964$	≤0.001[b]	0.956	1.000

Key: ANOVA, analysis of variance; ACA, anterior cingulate area; CAA, cortical amygdalar area; dfd (N-G), degrees of freedom denominator; dfn (G-1), degrees of freedom numerator; EA, entorhinal area; HB, hindbrain; HR, hippocampal region; IC, isocortex; MB, midbrain; mPFC, medial prefrontal cortex; NA, nucleus accumbens; OA, olfactory area; Partial η^2, an estimate of effect size; PPA, posterior parietal area; PPC, posterior parietal cortex; RA, retrosplenial area.
Repeated measures ANOVAs were used for statistical analyses.

[a] $p < 0.05$.

[b] $p < 0.01$.

[c] The "between groups' *p*-values" show *p*-values for the between-group comparisons.

[d] The "significant main effects" indicate the statistical results of a significant main effect for every measure.

et al., 2009). Given our findings and current evidence demonstrating neuropathological changes under HPA axis dysregulation and/or the AD process, future studies are required to unveil how the PS alters motor behavior in an appropriate APP mouse model.

4.3. The PS led to an earlier onset and overproduction of the Aβ plaques

Current lines of evidence from laboratories and clinics worldwide support the notion that an imbalance between production and clearance of $A\beta_{42}$ and related Aβ peptides is a very early, often initiating factor in AD (Fang et al., 2018; Selkoe and Hardy, 2016). In our study, the PS accelerated the appearance of Aβ plaques by 2–3 months as it induced a significant number of plaques, especially in cortical areas at 2 months, whereas the control animals began to show Aβ plaques at 4 months. Both groups displayed a remarkable development of plaques at 6 months, although the PA and largest plaque size were significantly larger across age in the PS group than the CG. Among specific brain regions selected for further analysis, FP, OA, ACA, PPA, and RE were the first brain areas that exhibited a higher PA in the PS group than the CG at 2 months. Other areas, that is, NA, HR, CAA, entorhinal area, MB, and HB, began to show a significant difference later at 4 months. The results were also sex specific, being higher in the female stress group. Our findings in PS overproduction of Aβ plaques, which were consistent with the behavioral measures of cognition, were congruent with contemporary laboratory and clinical evidence that supports the major impact of the $A\beta_{42}$ overproduction in early signs and progression of AD (Selkoe and Hardy, 2016). Although reduced synapse number has long been recognized as likely the strongest quantitative neuropathological correlate of the AD, experimental studies have shown that soluble oligomers of $A\beta_{42}$ isolated from the brains of patients with AD impair synapse number, inhibit long-term potentiation, and enhance long-term synaptic depression in rodent hippocampus, and injecting them into healthy rats impairs memory (Shankar et al., 2008). Even in postmortem brain tissue of subjects who were clinically mildly demented shortly before death, the higher oligomer-to-plaque ratio has been revealed than the nondemented controls (Esparza et al., 2013).

Previous studies with different experimental stress paradigms in adult AD mice also have shown that a repeated stress can result in a significant increase in Aβ soluble oligomers, exacerbate Aβ aggregation (Cuadrado-Tejedor et al., 2012; Marcello et al., 2012), impair neurotrophic signaling (Rothman et al., 2012), increase levels of tumor necrosis factor α and receptor for advanced glycation end products in the hippocampus (Cui et al., 2015), cause a progressive loss of hippocampal synapses (Marcello et al., 2012), and lead to disrupted function of the memory networks (Baglietto-Vargas et al., 2015). Stress has been found to modulate the earliest phases of the AD pathogenic process through increasing the levels of β-secretase BACE and the APP C-terminal fragments which infer from β/α-secretase cleavage (Baglietto-Vargas et al., 2015). PS studies also have shown an increase in hippocampal soluble Aβ (Martisova et al., 2013) and a higher vulnerability of female offspring to cognitive impairment (Fang et al., 2018). In a study on APPswe/PS1dE9 mice, higher levels of hippocampal proBDNF and soluble Aβ were observed in female control animals compared with their male littermates, and PS created a hippocampal decrease in mBDNF protein levels only in females. These findings may suggest an underlying role for BDNF signaling and Aβ production in higher susceptibility of females for AD development (Fukumoto et al., 2010; Sierksma et al., 2012). In addition, the stress-related Aβ aggregation is CRH

Table 7
Statistical results of probing the interaction between age and PS in all measures

Behavioural Tests and Brain Measurements	Significant main effects				
	F	df	*p*	η^2	Power
Corticosterone levels (ng/mL)	9.201	11	≤0.001[b]	0.574	1.000
Age	2.541	2	0.034[a]	0.086	0.642
Groups	28.734	3	≤0.001[b]	0.535	1.000
Age * groups	0.776	6	0.591	0.058	0.289
PPI of the ASR test					
ASR amplitude (%)	34.990	9	≤0.001[b]	0.623	1.000
Age	72.618	4	≤0.001[b]	0.615	1.000
Groups	2.262	1	0.134	0.007	0.323
Age * groups	0.043	4	1.000	0.001	0.061
PPI amplitude (%)	61.010	9	≤0.001[b]	0.749	1.000
Age	104.799	4	≤0.001[b]	0.705	1.000
Groups	92.877	1	≤0.001[b]	0.232	1.000
Age * groups	3.234	4	0.003[b]	0.069	0.953
ASR latency (ms)	52.096	9	≤0.001[b]	0.733	1.000
Age	106.401	4	≤0.001[b]	0.723	1.000
Groups	2.891	1	0.090	0.010	0.396
Age * groups	0.110	4	0.998	0.003	0.079
PPI latency (ms)	137.521	9	≤0.001[b]	0.872	1.000
Age	265.435	4	≤0.001[b]	0.860	1.000
Groups	79.176	1	≤0.001[b]	0.208	1.000
Age * groups	1.493	4	0.169	0.033	0.625
NOR test					
New object time (s)	8.493	5	≤0.001[b]	0.290	1.000
Age	11.363	2	≤0.001[b]	0.179	0.992
Groups	21.965	1	≤0.001[b]	0.174	0.996
Age * groups	0.552	2	0.577	0.011	0.139
Old object time (s)	9.393	5	≤0.001[b]	0.311	1.000
Age	18.468	2	≤0.001[b]	0.262	1.000
Groups	5.754	1	0.018[a]	0.052	0.662
Age * groups	0.170	2	0.844	0.003	0.076
NOR ratio	8.059	5	≤0.001[b]	0.279	1.000
Age	2.374	2	0.098	0.044	0.470
Groups	32.836	1	≤0.001[b]	0.240	1.000
Age * groups	3.399	2	0.037[a]	0.061	0.628
EPM test					
Open arm time (s)	7.083	5	≤0.001[b]	0.252	0.998
Age	0.519	2	0.597	0.010	0.134
Groups	29.336	1	≤0.001[b]	0.218	1.000
Age * groups	6.051	2	0.003[b]	0.103	0.876
Closed arm time (s)	52.317	5	≤0.001[b]	0.714	1.000
Age	0.598	2	0.552	0.011	0.147
Groups	218.448	1	≤0.001[b]	0.675	1.000
Age * groups	58.683	2	≤0.001[b]	0.528	1.000
EPM ratio	9.609	5	≤0.001[b]	0.314	1.000
Age	0.460	2	0.632	0.009	0.123
Groups	30.991	1	≤0.001[b]	0.228	1.000
Age * groups	12.730	2	≤0.001[b]	0.195	0.996
Rotarod test					
8 rpm speed (s)	5.782	5	≤0.001[b]	0.216	0.992
Age	11.203	2	≤0.001[b]	0.176	0.991
Groups	4.631	1	0.034[a]	0.042	0.568
Age * groups	2.423	2	0.094	0.044	0.479
16 rpm speed (s)	4.347	5	0.001[b]	0.172	0.958
Age	4.609	2	0.012[a]	0.081	0.769
Groups	10.682	1	0.001[b]	0.092	0.899
Age * groups	2.863	2	0.058	0.050	0.554
BBT					
Latency (s)	7.354	5	≤0.001[b]	0.259	0.999
Age	5.094	2	0.008[b]	0.088	0.811
Groups	19.337	1	≤0.001[b]	0.156	0.992
Age * groups	6.724	2	0.002[b]	0.114	0.910
Number of foot slips	32.689	5	≤0.001[b]	0.609	1.000
Age	16.129	2	≤0.001[b]	0.235	0.999
Groups	104.579	1	≤0.001[b]	0.499	1.000
Age * groups	30.107	2	≤0.001[b]	0.364	1.000
MWT					
Latency (s)	13.798	5	≤0.001[b]	0.020	1.000
Age	13.926	2	≤0.001[b]	0.008	0.998
Groups	43.079	1	≤0.001[b]	0.012	1.000
Age * groups	5.530	2	0.004[b]	0.003	0.854
Probe time (%)	4.104	5	0.002[b]	0.156	0.947
Age	2.640	2	0.076	0.045	0.515
Groups	16.029	1	≤0.001[b]	0.126	0.978
Age * groups	1.303	2	0.276	0.023	0.277

(*continued on next page*)

Table 7 (*continued*)

Behavioural Tests and Brain Measurements	Significant main effects				
	F	df	*p*	η^2	Power
Aβ plaque quantifications					
A1					
Total plaque area (%)	105.661	15	≤0.001[b]	0.877	1.000
Age	206.670	3	≤0.001[b]	0.856	1.000
Groups	118.089	3	≤0.001[b]	0.532	1.000
Age * groups	0.510	9	0.676	0.014	0.151
FP (%)	114.425	15	≤0.001[b]	0.885	1.000
Age	237.912	3	≤0.001[b]	0.873	1.000
Groups	80.689	3	≤0.001[b]	0.437	1.000
Age * groups	2.183	9	0.094	0.059	0.541
OA (%)	70.237	15	≤0.001[b]	0.825	1.000
Age	121.556	3	≤0.001[b]	0.778	1.000
Groups	111.827	3	≤0.001[b]	0.518	1.000
Age * groups	5.055	9	0.003[b]	0.127	0.909
Size (μm)	181.702	15	≤0.001[b]	0.925	1.000
Age	348.060	3	≤0.001[b]	0.910	1.000
Groups	195.011	3	≤0.001[b]	0.654	1.000
Age * groups	11.336	9	≤0.001[b]	0.248	0.999
A2					
Total plaque area (%)	88.198	15	≤0.001[b]	0.856	1.000
Age	162.661	3	≤0.001[b]	0.824	1.000
Groups	127.571	3	≤0.001[b]	0.551	1.000
Age * groups	0.610	9	0.610	0.017	0.173
IC (%)	145.963	15	≤0.001[b]	0.908	1.000
Age	262.009	3	≤0.001[b]	0.883	1.000
Groups	227.825	3	≤0.001[b]	0.687	1.000
Age * groups	2.230	9	0.064	0.071	0.629
Size (μm)	195.805	15	≤0.001[b]	0.931	1.000
Age	398.888	3	≤0.001[b]	0.921	1.000
Groups	150.481	3	≤0.001[b]	0.596	1.000
Age * groups	7.775	9	≤0.001[b]	0.186	0.987
A3					
Total plaque area (%)	226.077	15	≤0.001[b]	0.938	1.000
Age	472.179	3	≤0.001[b]	0.932	1.000
Groups	158.138	3	≤0.001[b]	0.603	1.000
Age * groups	2.622	9	0.055	0.070	0.628
ACA (%)	83.380	15	≤0.001[b]	0.849	1.000
Age	165.582	3	≤0.001[b]	0.827	1.000
Groups	75.334	3	≤0.001[b]	0.420	1.000
Age * groups	3.859	9	0.012[a]	0.100	0.810
NA (%)	86.747	15	≤0.001[b]	0.854	1.000
Age	161.848	3	≤0.001[b]	0.824	1.000
Groups	93.620	3	≤0.001[b]	0.474	1.000
Age * groups	9.354	9	≤0.001[b]	0.212	0.996
Size (μm)	231.733	15	≤0.001[b]	0.940	1.000
Age	483.225	3	≤0.001[b]	0.933	1.000
Groups	152.172	3	≤0.001[b]	0.594	1.000
Age * groups	6.762	9	≤0.001[b]	0.163	0.972
A4					
Total plaque area (%)	204.227	15	≤0.001[b]	0.932	1.000
Age	426.000	3	≤0.001[b]	0.925	1.000
Groups	130.628	3	≤0.001[b]	0.557	1.000
Age * groups	6.987	9	≤0.001[b]	0.168	0.976
PPA (%)	114.711	15	≤0.001[b]	0.885	1.000
Age	238.805	3	≤0.001[b]	0.873	1.000
Groups	83.990	3	≤0.001[b]	0.447	1.000
Age * groups	0.858	9	0.466	0.024	0.231
HR (%)	246.694	15	≤0.001[b]	0.943	1.000
Age	511.244	3	≤0.001[b]	0.936	1.000
Groups	151.281	3	≤0.001[b]	0.593	1.000
Age * groups	13.948	9	≤0.001[b]	0.287	1.000
Size (μm)	267.003	15	≤0.001[b]	0.948	1.000
Age	549.169	3	≤0.001[b]	0.942	1.000
Groups	186.141	3	≤0.001[b]	0.646	1.000
Age * groups	11.041	9	≤0.001[b]	0.245	0.999
A5					
Total plaque area (%)	197.492	15	≤0.001[b]	0.930	1.000
Age	421.787	3	≤0.001[b]	0.924	1.000
Groups	99.416	3	≤0.001[b]	0.489	1.000
Age * groups	5.889	9	0.001[b]	0.145	0.948
RA (%)	150.553	15	≤0.001[b]	0.910	1.000
Age	304.071	3	≤0.001[b]	0.898	1.000

Table 7 (*continued*)

Behavioural Tests and Brain Measurements	Significant main effects				
	F	df	*p*	η^2	Power
Groups	127.009	3	≤0.001[b]	0.550	1.000
Age * groups	4.883	9	0.003[b]	0.123	0.899
EA (%)	151.757	15	≤0.001[b]	0.911	1.000
Age	305.431	3	≤0.001[b]	0.898	1.000
Groups	115.624	3	≤0.001[b]	0.526	1.000
Age * groups	10.128	9	≤0.001[b]	0.226	0.998
CAA (%)	198.347	15	≤0.001[b]	0.930	1.000
Age	412.797	3	≤0.001[b]	0.923	1.000
Groups	124.318	3	≤0.001[b]	0.544	0.993
Age * groups	8.573	9	≤0.001[b]	0.198	1.000
Size (μm)	184.989	15	≤0.001[b]	0.927	1.000
Age	392.491	3	≤0.001[b]	0.920	1.000
Groups	106.912	3	≤0.001[b]	0.512	1.000
Age * groups	4.042	9	0.009[b]	0.106	0.829
A6					
Total plaque area (%)	281.423	15	≤0.001[b]	0.950	1.000
Age	607.550	3	≤0.001[b]	0.946	1.000
Groups	119.556	3	≤0.001[b]	0.535	1.000
Age * groups	9.251	9	≤0.001[b]	0.211	0.996
MB (%)	317.095	15	≤0.001[b]	0.955	1.000
Age	675.373	3	≤0.001[b]	0.951	1.000
Groups	144.883	3	≤0.001[b]	0.582	1.000
Age * groups	16.222	9	≤0.001[b]	0.319	1.000
HB (%)	345.265	15	≤0.001[b]	0.959	1.000
Age	756.975	3	≤0.001[b]	0.956	1.000
Groups	113.696	3	≤0.001[b]	0.522	1.000
Age * groups	10.745	9	≤0.001[b]	0.237	0.999
Size (μm)	140.196	15	≤0.001[b]	0.903	1.000
Age	277.571	3	≤0.001[b]	0.902	1.000
Groups	64.452	3	≤0.001[b]	0.417	1.000
Age * groups	0.438	9	0.647	0.010	0.119

Key: ANOVA, analysis of variance; ACA, anterior cingulate area; BBT, balance beam test; CAA, cortical amygdalar area; df, degrees of freedom; EA, entorhinal area; EPM, elevated plus maze; FP, frontal pole; HB, hindbrain; HR, hippocampal region; IC, isocortex; MB, midbrain; mPFC, medial prefrontal cortex; MWT, Morris water task; NA, nucleus accumbens; NOR, novel object recognition; OA, olfactory area; Partial η^2, an estimate of effect size; PPC, posterior parietal cortex; PPI of the ASR, prepulse inhibition of the acoustic startle reflex; RA, retrosplenial area.
Two-way ANOVAs were used for statistical analyses.
[a] $p < 0.05$.
[b] $p < 0.01$.

driven, wherein Aβ accumulates through CRH-dependent alterations of ɤ-secretase localization into lipid rafts and direct actions on ɤ-secretase (Marcello et al., 2015).

4.4. The PS was sex dependent in HPA-axis activity, learning function, and Aβ burden

Both animal studies and meta-analytic evidence of large populations in humans have indicated that females are more vulnerable for developing AD than males, and this increased incidence is not due to women having a longer lifespan (Carroll et al., 2010; Johansson et al., 2010; Laws et al., 2018). Given that ovarian hormones actively modulate a wide range of neuronal activities such as neural development and survival (McEwen, 2002; Simpkins et al., 2005; Wise, 2002) and promotion of neuron viability and reduction of Aβ aggregation (Pike et al., 2009), and estrogen-containing therapy has been remarkably successful in attenuating the risk for the AD progression in females early in menopause (Brinton, 2008), current evidence supports the major role of ovarian hormone decay on females' higher susceptibility to AD (Zhao et al., 2015). Consistently, rodent studies have indicated an increased Aβ deposition due to ovariectomy-induced hormone depletion in wild-type rodents (Petanceska et al., 2000) and some transgenic AD mouse models (Carroll et al., 2010; Levin-Allerhand et al., 2002; Zheng et al., 2002), and the positive effect of estradiol hormones in reducing these effects (Carroll et al., 2010). It is well-established that there is a reciprocal relationship between the HPA and hypothalamic-pituitary-gonadal axes, and hyperactivity of the stress axis, especially in persistent conditions, has an inhibitory effect on ovarian hormones secretion (Toufexis et al., 2014). Estrogen receptors also exist in 2 major subtypes, ERα and ERβ. It appears ERβ plays a greater role than ERα in mediating some estrogen-dependent neuroprotective actions, and ERβ genetic polymorphisms have shown to be associated with cognitive decline and increased vulnerability for AD in females (Zhao et al., 2015).

4.5. Study limitations and future directions

Although exposure to stress has been previously reported to impair cognitive performance in wild-type mice, the combination of stress with a genetic risk factor (overexpression of APP) could markedly aggravate the cognitive deficit (Marcello et al., 2015). For instance, in the study by Baglietto-Vargas et al., a short multimodal stress paradigm strongly affected only thin spines in wild-type mice, whereas caused a global decrease in the spine number in 3xTg-AD mice, suggesting spines in AD are more susceptible to stress (Baglietto-Vargas et al., 2015). Such observations imply more mechanistic investigations to figure out how stress modulates APP metabolism also in healthy conditions, as in wild-type mice, to further elucidate the contribution of environmental PS events in accelerating AD-like neuropathological deficits in offspring. In our study, wild-type littermates were not included. Thus, it is difficult to draw a conclusion whether PS exerted an exaggerated effect in these mice or if it was simply an additive.

This study aimed to investigate the neurobehavioral impacts of a repeated gestational noise stress paradigm on offspring during the

lifespan. We did not measure the CRH, GRs, and adrenocorticotropic hormone (ACTH) levels across age, which could provide further evidence for the dysregulation of the neuroendocrine system in response to PS. There are also several pathways in which stress exposure can regulate Aβ progression, like driving Aβ synthesis via the modulation of APP expression and the APP-cleaving secretases, or by modifying clearance of Aβ through changes in transportation to the periphery, or by modulating the rate of phagocytosis by immune cells (Hoeijmakers et al., 2018; Ries and Sastre, 2016). Studies suggest that both environmental noise and sensitivity to noise can affect health by producing changes in the immune response through increasing interleukin-12 levels and decreasing the population and activity of natural killer T cells (Kim et al., 2017). The propagation of tau neuropathology is also similarly modulated by tau expression, tau mutations, and activity of specific kinases and phosphatases due to long-lasting HPA-axis dysregulation (Chesser et al., 2013; Martin et al., 2013; Sanders et al., 2014). In future studies, quantifying the levels of the secretases, isoforms, C-terminal fragment, change in phosphorylated tau in plaque-associated dystrophic neurites, and also baseline immune activity and immune system alternations during lifespan are essential to provide further details of how the PS modifies APP processing in offspring.

Extensive evidence also indicates the contribution of HPA-axis dysregulation on the rodent hippocampal neuronal morphology, neural proliferation, and volume; medial prefrontal cortex volume, cell proliferation, and function; cortical thickness; and amygdala morphology and function (Jafari et al., 2018a; Kolb et al., 2012, 2013; Mychasiuk et al., 2012; Stewart and Kolb, 1988; Tata and Anderson, 2010), which are suggested to be studied in AD mouse models of PS.

5. Conclusions

In our study, the PS created a long-lasting dysregulation of the HPA axis, impaired performance in all cognitive and motor tasks, accelerated the onset age of showing Aβ pathology, and resulted in an overproduction of Aβ plaques during the lifespan. The PS-induced HPA-axis hyperactivity, deficit in spatial learning, and increased Aβ accumulation were sex specific and consistent with extensive evidence showing females' higher susceptibility for developing the AD. The findings imply the negative impacts of an enduring PS-induced HPA-axis hyperactivity on cognitive and motor behavior and precipitating the onset and progression of Aβ pathology in our mouse model of the AD. Future studies should probe concurrent alternations in levels of CRH, catecholamines, neurotransmitters, and neurotrophic factors across age.

Disclosure

The authors declare no conflict of interest.

Acknowledgements

The authors would like to acknowledge Di Shao for animal husbandry, Gerlinde A.S. Metz for using her lab equipment for the PPI of the ASR test, and Takashi Saito and Takaomi C Saido from RIKEN Brain Science Institute for providing the AD mice used in this study. This study was supported by Natural Sciences and Engineering Research Council of Canada (NSERC) Discovery Grant #40352, Alberta Innovates (CAIP Chair), Alberta Alzheimer Research Program, and Alzheimer Society of Canada to MHM; and a Canadian Institute for Advanced Research grant to BEK. This study was part of a postdoctoral fellowship to ZJ in Canadian Center for Behavioral Neuroscience (CCBN) at the University of Lethbridge.

Authors' contributions: ZJ, BEK, and MHM conceived and designed the method, and prepared and reviewed the article; ZJ performed experimental work and data analysis; MO assisted for brain slicing; HK helped in performing some behavioral tests; JM assisted for the corticosterone assay, and MHM and BEK provided project leadership.

Appendix A. Supplementary data

Supplementary data to this article can be found online at https://doi.org/10.1016/j.neurobiolaging.2019.01.019.

References

Abbott, P.W., Gumusoglu, S.B., Bittle, J., Beversdorf, D.Q., Stevens, H.E., 2018. Prenatal stress and genetic risk: how prenatal stress interacts with genetics to alter risk for psychiatric illness. Psychoneuroendocrinology 90, 9–21.

Ahima, R.S., Harlan, R.E., 1990. Charting of type II glucocorticoid receptor-like immunoreactivity in the rat central nervous system. Neuroscience 39, 579–604.

Angiolini, E., Fowden, A., Coan, P., Sandovici, I., Smith, P., Dean, W., Burton, G., Tycko, B., Reik, W., Sibley, C., Constancia, M., 2006. Regulation of placental efficiency for nutrient transport by imprinted genes. Placenta 27, S98–S102.

Antonelli, M.C., Pallares, M.E., Ceccatelli, S., Spulber, S., 2017. Long-term consequences of prenatal stress and neurotoxicants exposure on neurodevelopment. Prog. Neurobiol. 155, 21–35.

Autry, A.E., Monteggia, L.M., 2012. Brain-derived neurotrophic factor and neuropsychiatric disorders. Pharmacol. Rev. 64, 238–258.

Baglietto-Vargas, D., Chen, Y., Suh, D., Ager, R.R., Rodriguez-Ortiz, C.J., Medeiros, R., Myczek, K., Green, K.N., Baram, T.Z., LaFerla, F.M., 2015. Short-term modern life-like stress exacerbates Abeta-pathology and synapse loss in 3xTg-AD mice. J. Neurochem. 134, 915–926.

Bailoo, J.D., Varholick, J.A., Garza, X.J., Jordan, R.L., Hintze, S., 2016. Maternal separation followed by isolation-housing differentially affects prepulse inhibition of the acoustic startle response in C57BL/6 mice. Dev. Psychobiol. 58, 937–944.

Bakshi, V.P., Alsene, K.M., Roseboom, P.H., Connors, E.E., 2012. Enduring sensorimotor gating abnormalities following predator exposure or corticotropin-releasing factor in rats: a model for PTSD-like information-processing deficits? Neuropharmacology 62, 737–748.

Barlow, S.M., Knight, A.F., Sullivan, F.M., 1978. Delay in postnatal growth and development of offspring produced by maternal restraint stress during pregnancy in the rat. Teratology 18, 211–218.

Basner, M., Babisch, W., Davis, A., Brink, M., Clark, C., Janssen, S., Stansfeld, S., 2014. Auditory and non-auditory effects of noise on health. Lancet 383, 1325–1332.

Bellucci, A., Luccarini, I., Scali, C., Prosperi, C., Giovannini, M.G., Pepeu, G., Casamenti, F., 2006. Cholinergic dysfunction, neuronal damage and axonal loss in TgCRND8 mice. Neurobiol. Dis. 23, 260–272.

Belnoue, L., Malvaut, S., Ladeveze, E., Abrous, D.N., Koehl, M., 2016. Plasticity in the olfactory bulb of the maternal mouse is prevented by gestational stress. Sci. Rep. 6, 37615.

Bisht, K., El Hajj, H., Savage, J.C., Sanchez, M.G., Tremblay, M.E., 2016. Correlative Light and Electron Microscopy to Study Microglial Interactions with beta-Amyloid Plaques. J. Vis. Exp. 112.

Bock, J., Wainstock, T., Braun, K., Segal, M., 2015. Stress in utero: prenatal programming of brain plasticity and cognition. Biol. Psychiatry 78, 315–326.

Brinton, R.D., 2008. The healthy cell bias of estrogen action: mitochondrial bioenergetics and neurological implications. Trends Neurosci. 31, 529–537.

Burgado, J., Harrell, C.S., Eacret, D., Reddy, R., Barnum, C.J., Tansey, M.G., Miller, A.H., Wang, H., Neigh, G.N., 2014. Two weeks of predatory stress induces anxiety-like behavior with co-morbid depressive-like behavior in adult male mice. Behav. Brain Res. 275, 120–125.

Carroll, J.C., Rosario, E.R., Kreimer, S., Villamagna, A., Gentzschein, E., Stanczyk, F.Z., Pike, C.J., 2010. Sex differences in beta-amyloid accumulation in 3xTg-AD mice: role of neonatal sex steroid hormone exposure. Brain Res. 1366, 233–245.

Chang, T.Y., Beelen, R., Li, S.F., Chen, T.I., Lin, Y.J., Bao, B.Y., Liu, C.S., 2014. Road traffic noise frequency and prevalent hypertension in Taichung, Taiwan: a cross-sectional study. Environ. Health 13, 37.

Charil, A., Laplante, D.P., Vaillancourt, C., King, S., 2010. Prenatal stress and brain development. Brain Res. Rev. 65, 56–79.

Chesser, A.S., Pritchard, S.M., Johnson, G.V., 2013. Tau clearance mechanisms and their possible role in the pathogenesis of Alzheimer disease. Front. Neurol. 4, 122.

Clancy, B., Finlay, B.L., Darlington, R.B., Anand, K.J., 2007. Extrapolating brain development from experimental species to humans. Neurotoxicology 28, 931–937.

Conti, L.H., Murry, J.D., Ruiz, M.A., Printz, M.P., 2002. Effects of corticotropin-releasing factor on prepulse inhibition of the acoustic startle response in two rat strains. Psychopharmacology 161, 296–303.

Conti, L.H., Printz, M.P., 2003. Rat strain-dependent effects of repeated stress on the acoustic startle response. Behav. Brain Res. 144, 11–18.

Crocker, I., 2006. Cytokines, growth factors, placental insufficiency and infection. In: Baker, P., Sibley, C. (Eds.), The Placenta and Neurodisability. Mc Keith Press, London, pp. 44–57.
Cromwell, H.C., Atchley, R.M., 2015. Influence of emotional states on inhibitory gating: animals models to clinical neurophysiology. Behav. Brain Res. 276, 67–75.
Crudo, A., Petropoulos, S., Moisiadis, V.G., Iqbal, M., Kostaki, A., Machnes, Z., Szyf, M., Matthews, S.G., 2012. Prenatal synthetic glucocorticoid treatment changes DNA methylation states in male organ systems: multigenerational effects. Endocrinology 153, 3269–3283.
Cuadrado-Tejedor, M., Ricobaraza, A., Frechilla, D., Franco, R., Perez-Mediavilla, A., Garcia-Osta, A., 2012. Chronic mild stress accelerates the onset and progression of the Alzheimer's disease phenotype in Tg2576 mice. J. Alzheimers Dis. 28, 567–578.
Cui, B., Li, K., 2013. Chronic noise exposure and Alzheimer disease: is there an etiological association? Med. Hypotheses 81, 623–626.
Cui, B., Li, K., Gai, Z., She, X., Zhang, N., Xu, C., Chen, X., An, G., Ma, Q., Wang, R., 2015. Chronic noise exposure Acts Cumulatively to exacerbate Alzheimer's disease-like amyloid-beta pathology and neuroinflammation in the rat Hippocampus. Sci. Rep. 5, 12943.
Cui, B., Wu, M., She, X., Liu, H., 2012. Impulse noise exposure in rats causes cognitive deficits and changes in hippocampal neurotransmitter signaling and tau phosphorylation. Brain Res. 1427, 35–43.
De la Casa, L.G., Mena, A., Ruiz-Salas, J.C., 2016. Effect of stress and attention on startle response and prepulse inhibition. Physiol. Behav. 165, 179–186.
de Weerth, C., Buitelaar, J.K., 2005. Physiological stress reactivity in human pregnancy–a review. Neurosci. Biobehav. Rev. 29, 295–312.
Dineley, K.T., Xia, X., Bui, D., Sweatt, J.D., Zheng, H., 2002. Accelerated plaque accumulation, associative learning deficits, and up-regulation of alpha 7 nicotinic receptor protein in transgenic mice co-expressing mutant human presenilin 1 and amyloid precursor proteins. J. Biol. Chem. 277, 22768–22780.
Dong, E., Dzitoyeva, S.G., Matrisciano, F., Tueting, P., Grayson, D.R., Guidotti, A., 2015. Brain-derived neurotrophic factor epigenetic modifications associated with schizophrenia-like phenotype induced by prenatal stress in mice. Biol. Psychiatry 77, 589–596.
Esparza, T.J., Zhao, H., Cirrito, J.R., Cairns, N.J., Bateman, R.J., Holtzman, D.M., Brody, D.L., 2013. Amyloid-beta oligomerization in Alzheimer dementia versus high-pathology controls. Ann. Neurol. 73, 104–119.
Fameli, M., Kitraki, E., Stylianopoulou, F., 1994. Effects of hyperactivity of the maternal hypothalamic-pituitary-adrenal (HPA) axis during pregnancy on the development of the HPA axis and brain monoamines of the offspring. Int. J. Dev. Neurosci. 12, 651–659.
Fang, Y., Li, H., Chang, L., Song, Y., Ma, L., Lu, L., Du, Z., Li, Y., Liu, J., Wu, Y., 2018. Prenatal stress induced gender-specific alterations of N-methyl-d-aspartate receptor subunit expression and response to Abeta in offspring hippocampal cells. Behav. Brain Res. 336, 182–190.
Fride, E., Dan, Y., Feldon, J., Halevy, G., Weinstock, M., 1986. Effects of prenatal stress on vulnerability to stress in prepubertal and adult rats. Physiol. Behav. 37, 681–687.
Fukumoto, N., Fujii, T., Combarros, O., Kamboh, M.I., Tsai, S.J., Matsushita, S., Nacmias, B., Comings, D.E., Arboleda, H., Ingelsson, M., Hyman, B.T., Akatsu, H., Grupe, A., Nishimura, A.L., Zatz, M., Mattila, K.M., Rinne, J., Goto, Y., Asada, T., Nakamura, S., Kunugi, H., 2010. Sexually dimorphic effect of the Val66Met polymorphism of BDNF on susceptibility to Alzheimer's disease: new data and meta-analysis. Am. J. Med. Genet. B. Neuropsychiatr. Genet. 153b, 235–242.
Goldman, W.P., Baty, J.D., Buckles, V.D., Sahrmann, S., Morris, J.C., 1999. Motor dysfunction in mildly demented AD individuals without extrapyramidal signs. Neurology 53, 956–962.
Grace, T., Bulsara, M., Robinson, M., Hands, B., 2016. The impact of maternal gestational stress on motor development in late childhood and adolescence: a longitudinal study. Child Dev. 87, 211–220.
Harle, G., Lalonde, R., Fonte, C., Ropars, A., Frippiat, J.P., Strazielle, C., 2017. Repeated corticosterone injections in adult mice alter stress hormonal receptor expression in the cerebellum and motor coordination without affecting spatial learning. Behav. Brain Res. 326, 121–131.
Hefendehl, J.K., Wegenast-Braun, B.M., Liebig, C., Eicke, D., Milford, D., Calhoun, M.E., Kohsaka, S., Eichner, M., Jucker, M., 2011. Long-term in vivo imaging of beta-amyloid plaque appearance and growth in a mouse model of cerebral beta-amyloidosis. J. Neurosci. 31, 624–629.
Heffner, H.E., Heffner, R.S., 2007. Hearing ranges of laboratory animals. J. Am. Assoc. Lab. Anim. Sci. 46, 20–22.
Henry, C., Kabbaj, M., Simon, H., Le Moal, M., Maccari, S., 1994. Prenatal stress increases the hypothalamo-pituitary-adrenal axis response in young and adult rats. J. Neuroendocrinol. 6, 341–345.
Hoeijmakers, L., Lesuis, S.L., Krugers, H., Lucassen, P.J., Korosi, A., 2018. A preclinical perspective on the enhanced vulnerability to Alzheimer's disease after early-life stress. Neurobiol. Stress 8, 172–185.
Hoeijmakers, L., Ruigrok, S.R., Amelianchik, A., Ivan, D., van Dam, A.M., Lucassen, P.J., Korosi, A., 2017. Early-life stress lastingly alters the neuroinflammatory response to amyloid pathology in an Alzheimer's disease mouse model. Brain Behav. Immun. 63, 160–175.
Huizink, A.C., Mulder, E.J., Buitelaar, J.K., 2004. Prenatal stress and risk for psychopathology: specific effects or induction of general susceptibility? Psychol. Bull. 130, 115–142.
Jafari, Z., Faraji, J., Mirza Agha, B., Metz, G.A.S., Kolb, B.E., Mohajerani, M.H., 2017a. The adverse effects of auditory stress on mouse uterus receptivity and behaviour. Sci. Rep. 7, 4720.
Jafari, Z., Kolb, B.E., Mohajerani, M.H., 2017b. Effect of acute stress on auditory processing: a systematic review of human studies. Rev. Neurosci. 28, 1–13.
Jafari, Z., Kolb, B.E., Mohajerani, M.H., 2018a. Chronic traffic noise stress accelerates brain impairment and cognitive decline in mice. Exp. Neurol. 308, 1–12.
Jafari, Z., Mehla, J., Afrashteh, N., Kolb, B.E., Mohajerani, M.H., 2017c. Corticosterone response to gestational stress and postpartum memory function in mice. PLoS One 12, e0180306.
Jafari, Z., Mehla, J., Kolb, B.E., Mohajerani, M.H., 2017d. Prenatal noise stress impairs HPA axis and cognitive performance in mice. Sci. Rep. 7, 10560.
Jafari, Z., Mehla, J., Kolb, B.E., Mohajerani, M.H., 2018b. Gestational stress Augments postpartum β-amyloid pathology and cognitive decline in a mouse model of Alzheimer's disease. Cereb. Cortex. https://doi.org/10.1093/cercor/bhy251.
Jia, N., Li, Q., Sun, H., Song, Q., Tang, G., Sun, Q., Wang, W., Chen, R., Li, H., Zhu, Z., 2015. Alterations of group I mGluRs and BDNF associated with behavioral Abnormity in prenatally stressed offspring rats. Neurochem. Res. 40, 1074–1082.
Johansson, L., Guo, X., Waern, M., Ostling, S., Gustafson, D., Bengtsson, C., Skoog, I., 2010. Midlife psychological stress and risk of dementia: a 35-year longitudinal population study. Brain 133, 2217–2224.
Khalsa, D.S., 2015. Stress, Meditation, and Alzheimer's disease prevention: where the evidence Stands. J. Alzheimers Dis. 48, 1–12.
Kim, A., Sung, J.H., Bang, J.H., Cho, S.W., Lee, J., Sim, C.S., 2017. Effects of self-reported sensitivity and road-traffic noise levels on the immune system. PLoS One 12, e0187084.
Kim, E.J., Pellman, B., Kim, J.J., 2015. Stress effects on the hippocampus: a critical review. Learn. Mem. 22, 411–416.
Kjaer, S.L., Wegener, G., Rosenberg, R., Lund, S.P., Hougaard, K.S., 2010. Prenatal and adult stress interplay–behavioral implications. Brain Res. 1320, 106–113.
Koch, M., 1999. The neurobiology of startle reflex. Prog. Neurobiol. 59, 107–128.
Kolb, B., Mychasiuk, R., Muhammad, A., Gibb, R., 2013. Brain plasticity in the developing brain. Prog. Brain Res. 207, 35–64.
Kolb, B., Mychasiuk, R., Muhammad, A., Li, Y., Frost, D.O., Gibb, R., 2012. Experience and the developing prefrontal cortex. Proc. Natl. Acad. Sci. U. S. A. 109, 17186–17193.
Lalonde, R., Dumont, M., Staufenbiel, M., Strazielle, C., 2005. Neurobehavioral characterization of APP23 transgenic mice with the SHIRPA primary screen. Behav. Brain Res. 157, 91–98.
Laws, K.R., Irvine, K., Gale, T.M., 2018. Sex differences in Alzheimer's disease. Curr. Opin. Psychiatry 31, 133–139.
Levin-Allerhand, J.A., Lominska, C.E., Wang, J., Smith, J.D., 2002. 17Alpha-estradiol and 17beta-estradiol treatments are effective in lowering cerebral amyloid-beta levels in AbetaPPSWE transgenic mice. J. Alzheimers Dis. 4, 449–457.
Li, L., Du, Y., Li, N., Wu, X., Wu, Y., 2009. Top-down modulation of prepulse inhibition of the startle reflex in humans and rats. Neurosci. Biobehav. Rev. 33, 1157–1167.
Livingston, G., Sommerlad, A., Orgeta, V., Costafreda, S.G., Huntley, J., Ames, D., Ballard, C., Banerjee, S., Burns, A., Cohen-Mansfield, J., Cooper, C., Fox, N., Gitlin, L.N., Howard, R., Kales, H.C., Larson, E.B., Ritchie, K., Rockwood, K., Sampson, E.L., Samus, Q., Schneider, L.S., Selbaek, G., Teri, L., Mukadam, N., 2017. Dementia prevention, intervention, and care. Lancet 390, 2673–2734.
Maccari, S., Darnaudery, M., Morley-Fletcher, S., Zuena, A.R., Cinque, C., Van Reeth, O., 2003. Prenatal stress and long-term consequences: implications of glucocorticoid hormones. Neurosci. Biobehav. Rev. 27, 119–127.
Maccari, S., Piazza, P.V., Kabbaj, M., Barbazanges, A., Simon, H., Le Moal, M., 1995. Adoption reverses the long-term impairment in glucocorticoid feedback induced by prenatal stress. J. Neurosci. 15, 110–116.
Marcello, E., Epis, R., Saraceno, C., Di Luca, M., 2012. Synaptic dysfunction in Alzheimer's disease. Adv. Exp. Med. Biol. 970, 573–601.
Marcello, E., Gardoni, F., Di Luca, M., 2015. Alzheimer's disease and modern lifestyle: what is the role of stress? J. Neurochem. 134, 795–798.
Marlier, L.N., Csikos, T., Rebaudengo, N., Borboni, P., Patacchioli, F.R., Angelucci, L., Privat, A., Lauro, R., 1995. Distribution of glucocorticoid receptor mRNA in the rat spinal cord. Neuroreport 6, 2245–2249.
Martin, L., Latypova, X., Wilson, C.M., Magnaudeix, A., Perrin, M.L., Yardin, C., Terro, F., 2013. Tau protein kinases: involvement in Alzheimer's disease. Ageing Res. Rev. 12, 289–309.
Martisova, E., Aisa, B., Guerenu, G., Ramirez, M.J., 2013. Effects of early maternal separation on biobehavioral and neuropathological markers of Alzheimer's disease in adult male rats. Curr. Alzheimer Res. 10, 420–432.
McEwen, B., 2002. Estrogen actions throughout the brain. Recent Prog. Horm. Res. 57, 357–384.
Metz, G.A., 2007. Stress as a modulator of motor system function and pathology. Rev. Neurosci. 18, 209–222.
Metz, G.A., Jadavji, N.M., Smith, L.K., 2005. Modulation of motor function by stress: a novel concept of the effects of stress and corticosterone on behavior. Eur. J. Neurosci. 22, 1190–1200.
Mychasiuk, R., Gibb, R., Kolb, B., 2012. Prenatal stress alters dendritic morphology and synaptic connectivity in the prefrontal cortex and hippocampus of developing offspring. Synapse 66, 308–314.
Neigh, G.N., Nemeth, C.L., Kelly, S.D., Hardy, E.E., Bourke, C., Stowe, Z.N., Owens, M.J., 2017. Prenatal stress-induced increases in hippocampal von Willebrand factor expression are prevented by concurrent prenatal escitalopram. Physiol. Behav. 172, 24–30.

O'Keeffe, S.T., Kazeem, H., Philpott, R.M., Playfer, J.R., Gosney, M., Lye, M., 1996. Gait disturbance in Alzheimer's disease: a clinical study. Age Ageing 25, 313–316.
Ouis, D., 2001. Annoyance from road traffic noise: a review. J. Env. Psychol. 21, 101–120.
Paxinos, G., Franklin, K.B.J., 2001. The Mouse Brain in Stereotaxic Coordinates. Academic Press, San Diego, CA.
Petanceska, S.S., Nagy, V., Frail, D., Gandy, S., 2000. Ovariectomy and 17beta-estradiol modulate the levels of Alzheimer's amyloid beta peptides in brain. Exp. Gerontol. 35, 1317–1325.
Pike, C.J., Carroll, J.C., Rosario, E.R., Barron, A.M., 2009. Protective actions of sex steroid hormones in Alzheimer's disease. Front. Neuroendocrinol. 30, 239–258.
Ratajczak, P., Kus, K., Murawiecka, P., Slodzinska, I., Giermaziak, W., Nowakowska, E., 2015. Biochemical and cognitive impairments observed in animal models of schizophrenia induced by prenatal stress paradigm or methylazoxymethanol acetate administration. Acta Neurobiol. Exp. 75, 314–325.
Richter, S., Schulz, A., Zech, C.M., Oitzl, M.S., Daskalakis, N.P., Blumenthal, T.D., Schachinger, H., 2011. Cortisol rapidly disrupts prepulse inhibition in healthy men. Psychoneuroendocrinology 36, 109–114.
Ries, M., Sastre, M., 2016. Mechanisms of Abeta clearance and Degradation by glial cells. Front. Aging Neurosci. 8, 160.
Rohleder, C., Jung, F., Mertgens, H., Wiedermann, D., Sue, M., Neumaier, B., Graf, R., Leweke, F.M., Endepols, H., 2014. Neural correlates of sensorimotor gating: a metabolic positron emission tomography study in awake rats. Front. Behav. Neurosci. 8, 178.
Rohleder, C., Wiedermann, D., Neumaier, B., Drzezga, A., Timmermann, L., Graf, R., Leweke, F.M., Endepols, H., 2016. The functional networks of prepulse inhibition: neuronal connectivity analysis based on FDG-PET in awake and Unrestrained rats. Front. Behav. Neurosci. 10, 148.
Rothman, S.M., Herdener, N., Camandola, S., Texel, S.J., Mughal, M.R., Cong, W.N., Martin, B., Mattson, M.P., 2012. 3xTgAD mice exhibit altered behavior and elevated Abeta after chronic mild social stress. Neurobiol. Aging 33, 830.e1–830.e12.
Saar, G., Cheng, N., Belluscio, L., Koretsky, A.P., 2015. Laminar specific detection of APP-induced neurodegeneration and recovery using MEMRI in an olfactory based Alzheimer's disease mouse model. NeuroImage 118, 183–192.
Saito, T., Matsuba, Y., Mihira, N., Takano, J., Nilsson, P., Itohara, S., Iwata, N., Saido, T.C., 2014. Single App knock-in mouse models of Alzheimer's disease. Nat. Neurosci 17, 661–663.
Saito, T., Matsuba, Y., Yamazaki, N., Hashimoto, S., Saido, T.C., 2016. Calpain activation in Alzheimer's model mice is an Artifact of APP and presenilin overexpression. J. Neurosci. 36, 9933–9936.
Sanders, D.W., Kaufman, S.K., DeVos, S.L., Sharma, A.M., Mirbaha, H., Li, A., Barker, S.J., Foley, A.C., Thorpe, J.R., Serpell, L.C., Miller, T.M., Grinberg, L.T., Seeley, W.W., Diamond, M.I., 2014. Distinct tau prion strains propagate in cells and mice and define different tauopathies. Neuron 82, 1271–1288.
Sandman, C.A., Glynn, L., Schetter, C.D., Wadhwa, P., Garite, T., Chicz-DeMet, A., Hobel, C., 2006. Elevated maternal cortisol early in pregnancy predicts third-trimester levels of placental corticotropin-releasing hormone (CRH): priming the placental clock. Peptides 27, 1457–1463.
Sasaguri, H., Nilsson, P., Hashimoto, S., Nagata, K., Saito, T., De Strooper, B., Hardy, J., Vassar, R., Winblad, B., Saido, T.C., 2017. APP mouse models for Alzheimer's disease preclinical studies. EMBO J. 36, 2473–2487.
Scarmeas, N., Hadjigeorgiou, G.M., Papadimitriou, A., Dubois, B., Sarazin, M., Brandt, J., Albert, M., Marder, K., Bell, K., Honig, L.S., Wegesin, D., Stern, Y., 2004. Motor signs during the course of Alzheimer disease. Neurology 63, 975–982.
Selkoe, D.J., Hardy, J., 2016. The amyloid hypothesis of Alzheimer's disease at 25 years. EMBO Mol. Med. 8, 595–608.
Shankar, G.M., Li, S., Mehta, T.H., Garcia-Munoz, A., Shepardson, N.E., Smith, I., Brett, F.M., Farrell, M.A., Rowan, M.J., Lemere, C.A., Regan, C.M., Walsh, D.M., Sabatini, B.L., Selkoe, D.J., 2008. Amyloid-beta protein dimers isolated directly from Alzheimer's brains impair synaptic plasticity and memory. Nat. Med 14, 837–842.
Sierksma, A.S., Prickaerts, J., Chouliaras, L., Rostamian, S., Delbroek, L., Rutten, B.P., Steinbusch, H.W., van den Hove, D.L., 2013. Behavioral and neurobiological effects of prenatal stress exposure in male and female APPswe/PS1dE9 mice. Neurobiol. Aging 34, 319–337.
Sierksma, A.S., Vanmierlo, T., De Vry, J., Raijmakers, M.E., Steinbusch, H.W., van den Hove, D.L., Prickaerts, J., 2012. Effects of prenatal stress exposure on soluble Abeta and brain-derived neurotrophic factor signaling in male and female APPswe/PS1dE9 mice. Neurochem. Int. 61, 697–701.
Simpkins, J.W., Yang, S.H., Wen, Y., Singh, M., 2005. Estrogens, progestins, menopause and neurodegeneration: basic and clinical studies. Cell Mol. Life Sci. 62, 271–280.
Stewart, J., Kolb, B., 1988. The effects of neonatal gonadectomy and prenatal stress on cortical thickness and asymmetry in rats. Behav. Neural Biol. 49, 344–360.
Su, Q., Zhang, H., Zhang, Y., Zhang, H., Ding, D., Zeng, J., Zhu, Z., Li, H., 2015. Maternal stress in gestation: birth outcomes and stress-related hormone response of the Neonates. Pediatr. Neonatol. 56, 376–381.
Suva, D., Favre, I., Kraftsik, R., Esteban, M., Lobrinus, A., Miklossy, J., 1999. Primary motor cortex involvement in Alzheimer disease. J. Neuropathol. Exp. Neurol. 58, 1125–1134.
Szuran, T.F., Pliska, V., Pokorny, J., Welzl, H., 2000. Prenatal stress in rats: effects on plasma corticosterone, hippocampal glucocorticoid receptors, and maze performance. Physiol. Behav. 71, 353–362.
Tamura, H., Ohgami, N., Yajima, I., Iida, M., Ohgami, K., Fujii, N., Itabe, H., Kusudo, T., Yamashita, H., Kato, M., 2012. Chronic exposure to low frequency noise at moderate levels causes impaired balance in mice. PLoS One 7, e39807.
Tata, D.A., Anderson, B.J., 2010. The effects of chronic glucocorticoid exposure on dendritic length, synapse numbers and glial volume in animal models: implications for hippocampal volume reductions in depression. Physiol. Behav. 99, 186–193.
Toufexis, D., Rivarola, M.A., Lara, H., Viau, V., 2014. Stress and the reproductive axis. J. Euroendocrinol. 26, 573–586.
Uno, H., Eisele, S., Sakai, A., Shelton, S., Baker, E., DeJesus, O., Holden, J., 1994. Neurotoxicity of glucocorticoids in the primate brain. Horm. Behav. 28, 336–348.
van Batenburg-Eddes, T., de Groot, L., Huizink, A.C., Steegers, E.A., Hofman, A., Jaddoe, V.W., Verhulst, F.C., Tiemeier, H., 2009. Maternal symptoms of anxiety during pregnancy affect infant neuromotor development: the generation R study. Dev. Neuropsychol. 34, 476–493.
Van den Bergh, B.R.H., van den Heuvel, M.I., Lahti, M., Braeken, M., de Rooij, S.R., Entringer, S., Hoyer, D., Roseboom, T., Raikkonen, K., King, S., Schwab, M., 2017. Prenatal developmental origins of behavior and mental health: the influence of maternal stress in pregnancy. Neurosci. Biobehav. Rev. [Epub ahead of print].
Wadhwa, P.D., Garite, T.J., Porto, M., Glynn, L., Chicz-DeMet, A., Dunkel-Schetter, C., Sandman, C.A., 2004. Placental corticotropin-releasing hormone (CRH), spontaneous preterm birth, and fetal growth restriction: a prospective investigation. Am. J. Obstet. Gynecol. 191, 1063–1069.
Wang, H., He, J., Zhang, R., Zhu, S., Wang, J., Kong, L., Tan, Q., Li, X.M., 2012. Sensorimotor gating and memory deficits in an APP/PS1 double transgenic mouse model of Alzheimer's disease. Behav. Brain Res. 233, 237–243.
Ward, H.E., Johnson, E.A., Salm, A.K., Birkle, D.L., 2000. Effects of prenatal stress on defensive withdrawal behavior and corticotropin-releasing factor systems in rat brain. Physiol. Behav. 70, 359–366.
Weinstock, M., 2017. Prenatal stressors in rodents: effects on behavior. Neurobiol. Stress 6, 3–13.
Weinstock, M., Matlina, E., Maor, G.I., Rosen, H., McEwen, B.S., 1992. Prenatal stress selectively alters the reactivity of the hypothalamic-pituitary-adrenal system in the female rat. Brain Res. 595, 195–200.
White, D.R., Boettcher, F.A., Miles, L.R., Gratton, M.A., 1998. Effectiveness of intermittent and continuous acoustic stimulation in preventing noise-induced hearing and hair cell loss. J. Acoust. Soc. Am. 103, 1566–1572.
Wilson, R.S., Bennett, D.A., Gilley, D.W., Beckett, L.A., Schneider, J.A., Evans, D.A., 2000. Progression of parkinsonian signs in Alzheimer's disease. Neurology 54, 1284–1289.
Wirths, O., Bayer, T.A., 2008. Motor impairment in Alzheimer's disease and transgenic Alzheimer's disease mouse models. Genes, Brain Behav. 7, 1–5.
Wise, P.M., 2002. Estrogens and neuroprotection. Trends Endocrinol. Metabol. 13, 229–230.
Young, J.B., 2002. Programming of sympathoadrenal function. Trends Endocrinol. Metabol. 13, 381–385.
Zhao, L., Woody, S.K., Chhibber, A., 2015. Estrogen receptor beta in Alzheimer's disease: from mechanisms to therapeutics. Ageing Res. Rev. 24, 178–190.
Zheng, H., Xu, H., Uljon, S.N., Gross, R., Hardy, K., Gaynor, J., Lafrancois, J., Simpkins, J., Refolo, L.M., Petanceska, S., Wang, R., Duff, K., 2002. Modulation of A(beta) peptides by estrogen in mouse models. J. Neurochemist. 80, 191–196.
Zijlmans, M.A., Riksen-Walraven, J.M., de Weerth, C., 2015. Associations between maternal prenatal cortisol concentrations and child outcomes: a systematic review. Neurosci. Biobehav. Rev. 53, 1–24.